ISSN 0256-4637
VOLUME 34 NUMBER 4 OCTOBER-DECEMBER 2012

Journal of Pure and Applied

Ultrasonics

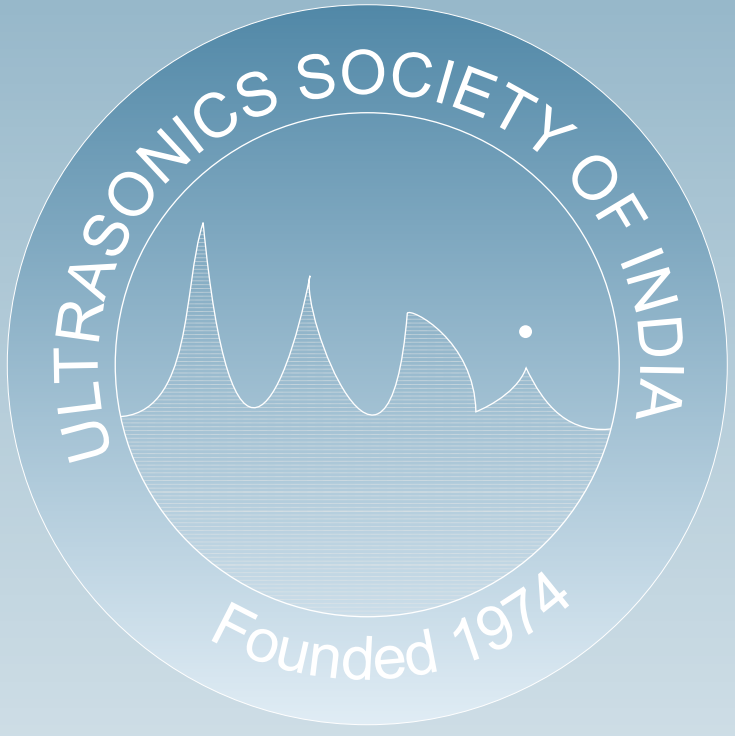

Website : www.ultrasonicsindia.com

A Publication of Ultrasonics Society of India

A Quarterly Publication of Ultrasonics Society of India

Journal of Pure and Applied

Ultrasonics

No. 4	Volume 34	October-December 2012

SUBSCRIPTION (postage paid)

Single	Rs. 550/-	US$ 50/-
Annual	Rs. 2200/-	US$ 200/-
USI	Free	

The submission of papers and all other correspondence regarding the Journal may please be addressed to :

Publication Secretary
Journal of Pure and Applied Ultrasonics
C/o Ultrasonics Society of India
National Physical Laboratory
Dr. K.S. Krishnan Road
New Delhi-110012

Journal of Pure and Applied Ultrasonics

VOLUME 34 NUMBER 4 OCTOBER-DECEMBER 2012

CONTENTS

Website : www.ultrasonicsindia.com

A Publication of — Ultrasonics Society of India

Information for authors

1. Type of Contribution

JOURNAL OF PURE AND APPLIED ULTRASONICS welcomes original research papers and articles related to the subject of ultrasonics. The contributions may be in the areas of physical ultrasonics, medical ultrasonics, ultrasonic non-destructive evaluation including NDT, high power ultrasonics, underwater acoustics, ultrasonic transducers, transducer materials & devices and any other related topic. These may fall into one of the following categories.

ResearchPapers **-** These should be on original research work contributing to scientific developments. They should be written with a wide readership in mind and should emphasize the significance of the work.

Reviews Articles **-** Includes critical reviews and survey articles.

Research and Technical notes **-** These should be short descriptions of new techniques, applications, instruments and components.

Letters to the editor **-** Letters will be published on points arising out of published articles and papers and on questions of opinion.

Miscellaneous **-** Miscellaneous contributions such as conference reports, Ph.D. thesis summaries and news items are also accepted. Recommended lengths of contributions are: Research papers 2000-4000 words, reviews articles 2000-5000 words; conference reports 500-1500 words; news items, research and technical notes up to 1000 words.

2. Manuscripts

Manuscripts should be typed on one side of the paper in double spacing with 25 mm margins on all side of A4 size paper. A soft copy of the manuscript in MS WORD for text and MS EXCEL for illustrations and a PDF file thereof may be sent by e-mail or CD/DVD. Colour images should be formatted as JPEG files. Figures submitted in colour would be publiashed in colour. Colour should be avoided unless it is required in order to convey a message or serve a purpose in the image.

Title **-** Titles should be short and indicate the nature of the contribution. About 5 keywords may be given after the abstract.

Abstract **-** An abstract of 100-200 words should be provided on the title page of paper and review article. This should describe the full scope of the contribution and include the principal conclusions.

Mathematics **-** Mathematical expressions should be arranged to occupy the minimum number of lines consistent with clarity e.g., $(x^2+y^2)/(x-y)^{1/2}$

References **-** References should be indicated in the text by its number only. The reference number should be given as superscript. The corresponding reference shall contain the following information in order; names and initials of author(s), full title of the work, journal or book title in italic, volume number, the year of publication in brackets and the page number. As example: Vasanth B.K., Palanichamy P., Jayakumar T. and Sankar B.N., Assessment of residual stresses in a carbon steel weld pad using critically refracted longitudinal (L_{CR}) waves, *J. Pure Appl. Ultrason.*, 28 (2006) 66-72.

Units and Abbreviations **-** Authors should use SI units wherever possible.

3. Reprints

One copy of the issue in which the paper is published is sent to the author free of charges.

J. Pure Appl. Ultrason. 34 (2012) pp. 69-71

Ultrasonic nondestructive characterisation of nuclear materials

K. Sakthipandi[1], V. Rajendran[1]* and T. Jayakumar[2],*

[1]Centre for Nano Science and Technology, K S Rangasamy College of Technology, Tiruchengode–637215, Tamil Nadu, India

[2]Indira Gandhi Centre for Atomic Research, Kalpakkam–603102, Tamil Nadu, India

Email : veerajendran@gmail.com

Ultrasonic non-destructive evaluation (NDE) technique is a versatile and sensitive tool for structural/microstructural and defect characterisation of materials. An indigenous experimental set-up developed in the authors' laboratory is used for on-line ultrasonic velocities and attenuation measurement over a wide range of temperatures from room temperature to 1100 K. The measured ultrasonic parameters such as ultrasonic velocities and derived elastic constants are used to assess changes in microstructural features as a function of temperatures. The first order differentials of the temperature dependent ultrasonic parameters are used to reveal the precise information about the structural/phase transitions. In the present investigation, ultrasonic longitudinal velocity measurements carried out in β-quenched Zircaloy-2 specimens in the temperature range of 298 to 623 K clearly reveal formation of intermetallic precipitates from the β-quenched martensite phase. It is observed that the first order differential plots of variation in ultrasonic velocity as function of temperature is an effective tool in predicting the temperatures at which the structural changes take place. In addition, the fatigue and the creep-fatigue damages in AISI 316 stainless steel are correlated with on-line ultrasonic velocity measurements, particularly made at elevated temperatures. The results reveal that in-situ high temperature ultrasonic measurements enable assessment of creep and fatigue damage with high sensitivity.

Keywords: Ultrasonic velocity, β-quenched Zircaloy-2, AISI 316 L (N) stainless steel

Introduction

With development of advanced technologies to characterise materials, materials evaluation is playing an even more significant role in alloy design, alloy development, process optimization and performance evaluation, for meeting the stringent and ever increasing service requirements for engineering applications[1-3]. Identification of microstructural variations during service conditions, and the influence of external environment of stress, temperature and chemical ambience on defect formation and progression are important parameters for both materials development as well as useful guideline to the design engineers to set acceptable limits for service conditions. While room temperature testing of simulated specimens is essential, there is little emphasis needed to highlight the role of on-line techniques towards enhancing the understanding of real time phase transitions and defect kinetics on material properties during service.

Ultrasonic characterization is a versatile and sensitive non-destructive tool, to explore not only the microstructural state of the material, but also to derive information about the defect state of the materials[4-5] The ultrasonic technique is a powerful tool for materials characterisation due to the well-developed basic understanding of the ultrasonic wave propagation, availability of the wide frequency ranges for the interaction of ultrasonic waves with macroscopic and microscope structural features with different scattering and absorption mechanisms, lattice defects etc. The ultrasonic materials characterisation is employed for the nuclear materials like AISI type 316, Stainless steel, Ziraloy–2 and 9 Cr–1Mo steel[6-7]. The measurements of temperature dependent ultrasonic longitudinal velocities in materials have been used to explore the physico-chemical properties, structural/phase changes, charge ordering, Curie temperature, Jahn-Teller temperature, phase transition temperature, metal insulator transition and grain size[8]. The first differentials of the temperature dependent ultrasonic parameters have been used as an effective tool to identify the structural/micro structural change in the materials [9]

*Life fellow : Ultrasonics Society of India

Experimental procedure

2.1. Ultrasonic velocity measurements

A high power ultrasonic Pulser Receiver (Olympus NDT, 5900 PR, USA) and a digital storage oscilloscope (DSO) (Lecroy, Wave Runner 104 MXi, 1GHz, USA) were employed for recording ultrasonic (rf) signals. The ultrasonic velocities for both the longitudinal and shear waves have been measured at a fundamental frequency of 5 MHz. An indigenously designed experimental set-up for high temperature ultrasonic velocity measurements has been employed using

the through transmission technique with waveguides (buffer rods)[9]. The measurements were made in the temperature range from 300 to 623 K with a slow rate of heating (1 K min^{-1}). The temperature has been controlled employing a programmable temperature controller (Eurotherm, 2604, USA). In the present experimental set-up, one can obtain the required temperature either by the dynamic mode or by the static mode depending on the requirements employing the Eurotherm temperature controller. The error in the measurement of temperature is ± 1 K. Precise transit time for the propagation of the ultrasonic waves into the calcinated (1000 °C 12 h) sample was measured by taking the difference in the transit times (Δt) between t_1 and t_2, where t_1 is the transit time measured only with buffer rods at a given temperature and t_2 is the transit time measured after introducing the sample in between the buffer rods, at the same temperature. Ultrasonic velocity (U_L/U_S) is determined using the relation[9]:

$$U = \frac{d}{\Delta t} \quad \ldots (1)$$

Knowing the sample thickness (d) in micron resolution and transit time (Δt) in nanosecond resolution, the overall accuracy obtained in the measurement of the velocity is ± 5 m s^{-1}.

Results and Discussion

Structural Features on Nuclear materials

The on-line measurements enabled in obtaining information on precipitation of hard intermetallic phases in β-quenched Zircaloy-2 subjected to different thermal treatments[10]. The temperature dependence of longitudinal wave velocity (U_L) and its first differentials for β-quenched Zircaloy-2 are represented in Fig. 1. The results obtained reveal interesting information about the microstructural changes taking place in β–quenched Ziraloy–2 specimen i.e., on-set of intermetallic precipitations at 573 K. The observed large magnitude in the peak at 573 K in the first differentials of ultrasonic longitudinal wave velocity against the temperature clearly indicates on-set of the intermetallic precipitations. In the β-quenched condition of the zircaloy-2, solute elements such as Sn, Fe, Ni and Cr are in the solid solution. During the aging process, the initiation of the formation of precipitation of hard intermetallic phases takes place from the supersaturated solid solution. The increases in the temperature of the aging up to 623 K lead to an increase in the hard intermetallic phases formed.

Further, the observed decrease in velocity with a increase in temperature can be explained in terms of the changes in the mean modulus brought about by the precipitates of hard intermetallics phases. Generally, in any materials, the volume fraction and the modulus of the individual phases contribute to the overall modulus[11]. The partial removal of elements like Sn, Fe, Ni and Cr from the matrix to form hard intermetallics during aging results in a change in the modulus. The volume fraction of the hard intermetallics is very small and hence, its contribution to the overall modulus is expected to be very small. Therefore, the net change in the modulus of the specimen is only due to the modulus of the matrix due to its altered compositional distribution (such as removal of Fe, Ni and Cr). A further reduction in the magnitude of the first differentials of U_L against the temperature has been observed; beyond 573 K. A small decrease in the magnitude of the first differentials of U_L with the temperature reveals the existence of hard intermetallic precipitations, as discussed elsewhere[11]

The temperature dependence of longitudinal wave velocity (U_L) and its first differentials for fatigue damaged (No. of cycles 301 with continuous cycling) and creep-fatigue damaged (No. of cycles 346, holding time 10 min.) austenitic 316 L(N) stainless steels are represented graphically in Figure 2. The observed reduction in velocity in creep-fatigue damaged specimen than in fatigue damaged specimen is due to the enhanced oxidation and creep damage at grain boundaries that accelerated the oxidation assisted transgranular fracture. This observed higher magnitude of decrease in velocity and larger variation in first differentials of velocity beyond 450 K reveals the potential of ultrasonic velocity measurements for an on-line monitoring of fatigue and the creep-fatigue damages that occur during the service life of the materials/components[12].

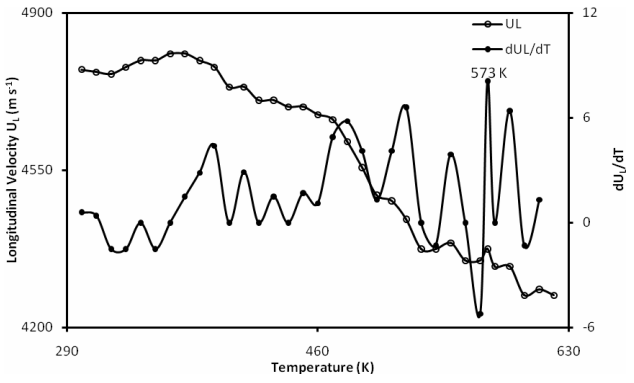

Fig. 1—Variation of the longitudinal wave velocity and first differential of longitudinal wave velocity in Ziraloy–2

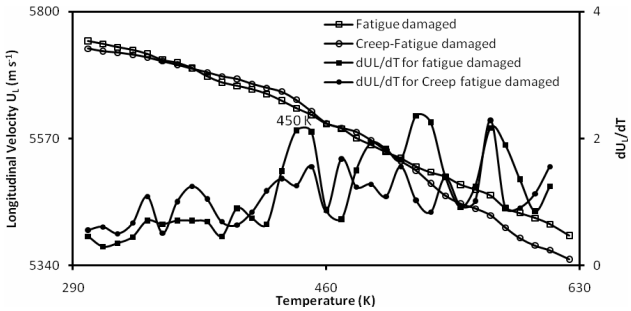

Fig. 2—Variation of the longitudinal wave velocity and first differential of longitudinal wave velocity in AISI 316 L (N) stainless steel

Conclusions

The followings are summary of these investigations:

1 The ultrasonic studies carried out in β-quenched zircaloy-2 reveal the formation of intermetallic precipitates at 573K.

2 The ultrasonic measurements carried out in AISI 316 stainless steel reveals the potential application of ultrasonic measurements for on-line monitoring of fatigue and creep-fatigue damages that occur beyond 450 K during the service life of the materials/compounds.

3 The first differential parameter of ultrasonic velocity is found to be a sensitive parameter to detect the early stages of microstructural and substructure variations in nuclear material.

4 The high temperature on-line ultrasonic characterisation technique combined with the first differential analysis of parameters makes the technique a unique high sensitive NDT technique to detect the temperature dependent phase, structural and properties changes in solid samples.

Acknowledgements

The authors (V. R and K. S) are thankful to Indira Gandhi Centre for Atomic Research (IGCAR), Kalpakkam for the financial support to carry out this research project (IGC/MMG/NDED/KSRCT/2008/2 dt. 16.04.2008).

References:

1 V.Rajendran, Baldev Raj and Palanichamy, 'Science and Technology of Ultrasonics', Narosa publication, New Delhi, 2004.

2 J. Schijve, Materials Science, Vol 39, No 3, pp 307-333, May 2003.

3 P. Yvon and F. Carre, Journal of Nuclear Materials, Vol 385, No 2, pp 217-222, March 2009.

4 J.F. Bussiene, Materials Evaluation, Vol 44, No 5, pp 560-567, April 1986.

5 P.Palanichamy, A. Joseph, T. Jayakumar, and Baldev Raj, NDT & E International, Vol 28, No 3, pp 179-185, Feburary 1995.

6 Baldevraj, S.L.Mannan, P.R.Vasudeve Rao, M.D. Mathew, Sadhana, Vol 27, Part 5, pp 527-558, October 2002.

7 M. Vasudevan and P.Palanichamy, Journal of Materials Engineering and Performance, Vol 11, No 2, pp 169-179, April 2002.

8 Nor Azah Nik Jaafar and R.Abd-Shukor, Physica B, Vol 334, Issue 3-4, pp 425-431 July 2003.

9 V.Rajendran K. Sakthipandi, T. Jayakumar, P.Palanichamy, P. Shankar and Baldev Raj, The Sixth International conference on condition Monitoring and Machinery Failure Prevention Technologies, Ireland pp. 1283-1295, June 2009.

10 A.Nisha Begam, V.Rajendran, T.Jayakumar, P.Palanichamy, N. Priyadharsini, S. Aravindan and Baldev Raj, "Material characterisation, Vol 58, pp 563-570, June 2007.

11 T. Jayakumar, P.Palanichamy and Baldev Raj, "Journal of Nuclear Materials, Vol 255, issue 2-3, pp 243-249, June 1998.

12 S. Muthukumaran, V. Rajendran, T. Jayakumar, P.Palanichamy, P. Shankar and Baldev Raj, Sciatica Material, pp.1234-39, September 2005.

J. Pure Appl. Ultrason. 34 (2012) pp 72-75

Ultrasonic properties of CuO nanoparticles based nanofluids

Vimal Pandey[1], S.K.Verma[2], R.R.Yadav*[2]

[1]Department of Physical Sciences, Mahatma Gandhi Chitrakoot Gramodaya Vishwavidyalaya, Chitrakoot, Satna (M. P.), India

[2]Department of Physics, University of Allahabad, Allahabad-211002, India
E-mail: rryadav1@rediffmail.com, vimal.71.alld@gmail.com

Study of nanofluids is important for different types of heat transfer management systems. Three different samples of CuO nanoparticles- PVA nanofluids are prepared through the chemical routes using ultrasonication. Temperature dependent ultrasonic velocity in the samples is measured and the behavior is correlated to extract the important information about thermal conduction at different temperatures. The results are applicable for the heat management in microelectronic industries.

Keywords: nanofluid; ultrasonic attenuation; ultrasonic velocity.

Introduction

Nanofluids have attracted the interest in recent years because of their enhanced thermal conductivity in comparison to the base fluids. Therefore, nanofluids can be used as a heat transfer fluid in the heat exchange systems[1]. The nanofluids are synthesized by dispersing a very small amount of nanoparticles having size in the range 10-100#nm in the base fluid like water, ethylene glycol, polyvinyl alcohol, polyvinyl pyrrolidone etc. using ultrasonication technique. The oxides of transition metal are an important class of semiconductors having applications in electronics, catalysis and solar energy transformation[2-9]. Among the oxides of transition metals, copper oxide nanoparticles are of special interest because of their wide use in catalysis, metallurgy and high temperature superconductors and as efficient as nanofluid in heat transfer application[10-12]. For example it has been reported that 4% addition of CuO improves the thermal conductivity of water by 20%[13]. This is a p-type semiconductor having monoclinic end centered crystal system. CuO nanoparticles have been fabricated by chemical route using various chemical precursors. In 1993, Hai-Yan *et al* published a method for synthesis of ultrafine CuO nanoparticles[14]. In 1988, Dianzeng et. al reported on a solid-state reaction between copper chloride and sodium hydroxide to prepare copper oxide nanoparticles having size of about 23 nm[15]. Later the same chemical process was repeated by Corrie *et. al* and reported formation of CuO nanoparticles in the range 7-9 nm[16]. Recently Fan et al reported synthesis of CuO nanocrystals using pyrolysis precipitation technique. In this technique chemical precursors decompose under suitable thermal treatment into solid compound and wastes are evaporated away. This paper describes the synthesis of CuO nanoparticles using sol-gel method followed by annealing at temperature 200°C#.The CuO nanoparticles obtained by annealing at 200°C were dispersed homogeneously in PVA using ultrasonicator (30 KHz, 500 Watt) to form nanofluid of required concentration. The particle size of the synthesized nanoparticles is measured by using XRD, TEM and acoustic attenuation spectroscopy (AAS) techniques. The sol-gel method chosen for the synthesis is better than pyrolysis precipitation method as this method leads to metal oxides having larger surface area and non symmetric nanocrystalline shapes with numerous edges, corners and defects that are advantageous in absorption and catalytic processes[16]. The ultrasonic velocity in nanofluids increases with temperature initially and becomes constant at higher temperatures[17]. The increase of ultrasonic velocity with increase in concentration is due to weakening of interaction between nanosized particle and micro sized fluid molecule and also due to decrease in density of nanofluid with increase of concentration[18].

*Life fellow, Ultrasonics Society of India

Presented at National Seminar on Materials characterization by Ultrasonics (NSMCU-2012), 3-4 April 2012, Amity school of Engineering & Technology Bijwasan, New Delhi.

Experimental details

Synthesis

3.0 g of copper (II) chloride was dissolved in 160 ml of ethanol. 1.8 g of sodium hydroxide was dissolved in 50 ml ethanol. The sodium hydroxide solution was added drop wise to copper (II) chloride solution with constant stirring at room temperature. As the reaction proceeds the colour of the solution turns from green to greenish blue and finally to black. The gel was filtered using centrifuge machine and washed with ethanol and water. In order to obtain copper oxide nanoparticles (CuO NPs) the sample of dried copper hydroxide gel was annealed at temperatures 200°C, 250°C, 300°C, 350°C, 400°C. Finally the annealed sample of copper oxide nanoparticles was grinded to get it in powdered form. An aqueous solution of concentration 4% of PVA was obtained by dissolving 10.0 g of PVA in 250ml water at 70°C with constant stirring for 2 hrs. CuO nanofluid of concentration 0.8 wt% was obtained by dissolving 0.8g of CuO NPs in 100ml of the prepared aqueous solution of PVA with the aid of ultrasonicator at room temperature.

Characterization

The XRD of powdered sample of CuO was recorded using a Philips P.W.1710 diffractometer with 0.15405 nm Cu K_α radiation. The average particle size (d) has been calculated from the line broadening in XRD pattern using Scherrer's formula: $d=0.9\lambda/\beta\cos\theta$, where λ is wavelength of X-ray, β is full width of half maximum (FWHM) and θ is Bragg's angle in radians. The TEM of CuO was performed with E.M.-C.M.-12 (Philips) transmission electron microscope operating at 200 KeV. APS-100 was used for the measurement of ultrasonic attenuation in the frequency range 48MHz to 99MHz and the data is used to determine the size of nanoparticles by ultrasonic spectroscopy.

Ultrasonic velocity measurement

Ultrasonic velocity over the temperature range 35°C-70°C was measured in the nanofluid samples having different concentration of CuO nanoparticles in PVA solution using multi-frequency interferometer at 3 MHz frequency. The temperature of the sample was maintained constant during the measurement using a thermostat and water circulation. The measured value of ultrasonic velocity is accurate to ± 0.1% with an error of measurement of ± 0.5°C in temperature.

Results and discussion

XRD pattern of the synthesized CuO NPs is shown in Figs. 1. On comparison of XRD with the data from JCPDS file no. 80-1917, the intensity and position of peaks of CuO NPs obtained by annealing at 200°C are in good agreement and its diffraction pattern can be recognized as monoclinic crystal system where as peaks in XRD of CuO NPs obtained by annealing at higher temperature are slightly displaced towards higher Bragg's angle. Lattice parameters of the unit cell of CuO are a =4.69 Å, b =3.43Å, c =5.13Å. The average

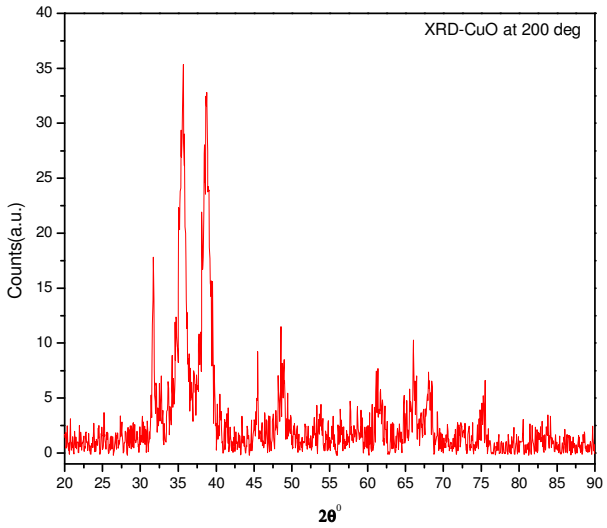

Fig. 1—D of CuO NPs at 200ºC

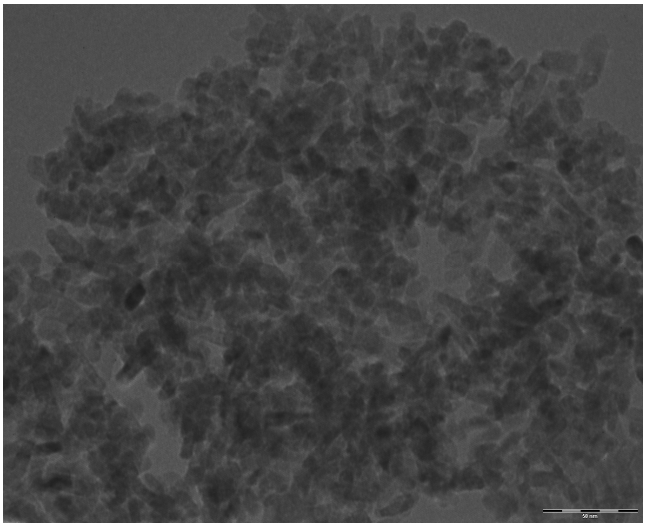

Fig. 2—EM image of CuO NPs

crystallite size of CuO NPs determined by the Scherrer formula is 16nm.

The TEM image of prepared nanoparticles is shown in Fig.2. The analysis of TEM image of CuO NPs confirms that the particle sizes of NPs lie in the range 10-16nm which is in good agreement with XRD analysis.

The plot of attenuation of ultrasonic wave in the nanofluid as a function of frequency in the range 48#MHz to 99#MHz is shown in Fig. 3. Figure 3 depicts that ultrasonic attenuation

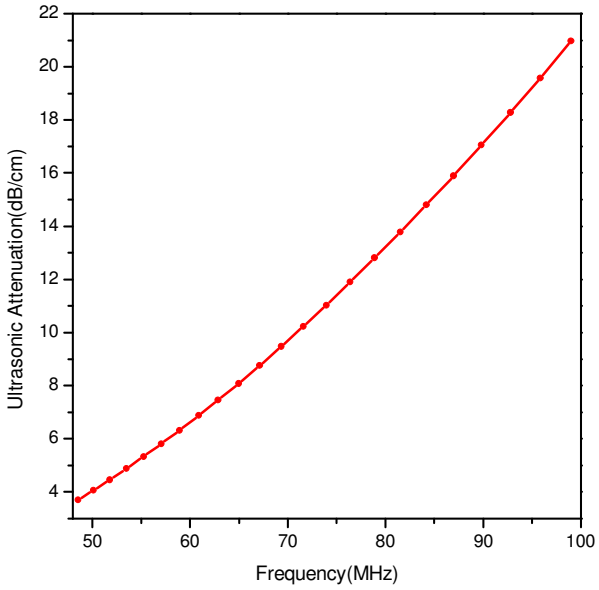

Fig.3—lot of ultrasonic attenuation versus frequency for CuO-PVA nanofluid

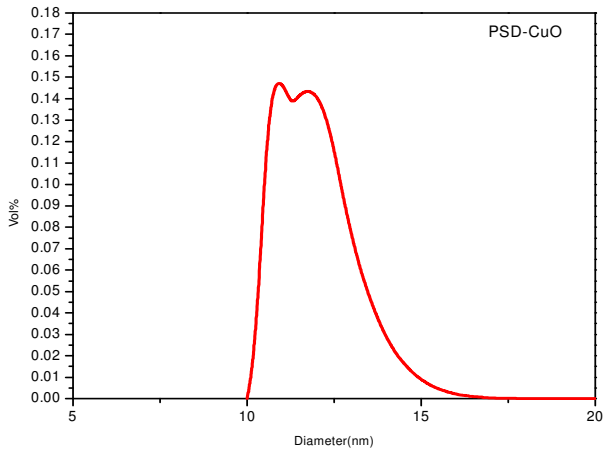

Fig. 4—article size distribution (PSD) of CuO NPs in PVA

increases with frequency of the ultrasonic wave. The attenuation curve can be interpreted as viscous drag loss and scattering loss are prominent due to similar thermal wavelength and particle size in this range. Thus frequency is the governing parameter to the attenuation in the present nanofluid. The ultrasonic attenuation data are inverted to particle size distribution (PSD) data. The plot of PSD of CuO NPs in the nanofluid determine by APS-100 is shown in Fig. 4. The PSD based on ultrasonic attenuation spectroscopy confirms that the particle sizes of CuO NPs lie in the range 10-17nm.

Ultrasonic velocity is highly dependent upon the size of the nanoparticles in nanofluid and on the temperature of the nanofluid, dispersion of the nanoparticles and density of the nanofluid. The results of the temperature dependent ultrasonic velocity at different concentrations are shown in Fig. 5. The perusal of plot reveals that the ultrasonic velocity in CuO –PVA nanofluid increases with temperature initially and becomes constant at higher temperatures. It is observed from the plot that the ultrasonic velocity in CuO-PVA nanofluid increases slightly with concentration in the measured range (0.2 wt %, 0.3 wt % and0.5 wt %), indicating that the nanofluids with small amount of nanoparticles are less compressible according to Newton-Laplace's relation for adiabatic compressibility: $\beta=1/\rho v^2$; where ρ is density of nanofluid and v is ultrasonic velocity in nanofluid. The cause behind this increase of ultrasonic velocity with increase in concentration is due to weakening of interaction between nanosized particle and micro sized fluid molecule and also due to decrease in density of nanofluid with increase of concentration.

It is also observed from the plot that ultrasonic velocity in nanofluid increases with temperature nonlinearly. The temperature dependency of ultrasonic velocity for liquids is $V=V_0+V_1T$ (V_0 is ultrasonic velocity at 273^0K, V_1 is temperature gradient of velocity and T is temperature rise from 273°K). The ultrasonic velocity in liquids generally decreases with temperature due to having negative temperature gradient of velocity. The anomalous behavior of velocity can

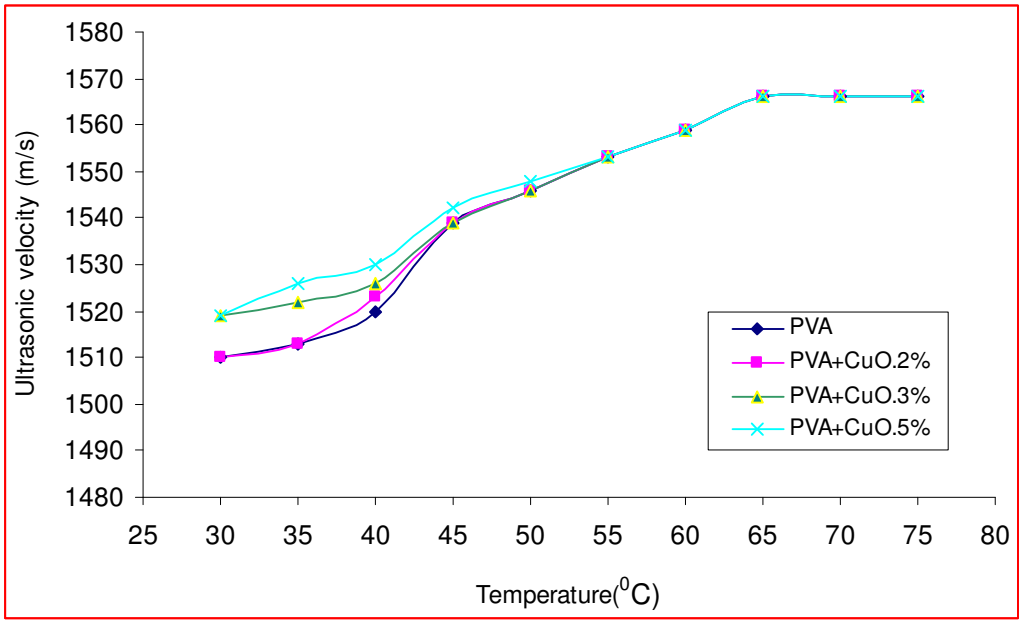

Fig.5—ltrasonic velocity vs temperature at different concentrations

be interpreted as the nanosized CuO particles has more surface to volume ratio and formation of hydrogen bonds with PVA molecules can absorb more PVA molecules on its surface, hence making the transport easy from one point to another point, which enhances the velocity.

References:

1 G Mishra, S.K. Verma, D. Singh, P.K. Yadawa, R.R. Yadav, Open J. of Acoust., 1 (2011) 9.

2 A.S. Lane, R.S. Ningthoujam, S.J. Sharma, R.K. Vatsa, R.B. Pode, Int. Jour. Of Nanotech., 7 (2010) 979.

3 T. Mitsuyu, O. Yamakazi, K. Ohji, K.Wasa, Ferroelectrics, 42 (1982) 233.

4 O. Regan, M. Gratzel, Nature, 353 (1991) 737.

5 K. Naazeeruddin, A. Kay, M. Gratzel, J. Am. Chem. Soc., 115 (1993) 6832.

6 U. Bjoerksten, J. Moser, M. Gratzel, Chem. Mater., 6 (1994) 858.

7 W.P. Dow, T.J. Huang, J. Catal., 160 (1996) 171.

8 P.O. Larsson, A. Andersson, R.L. Wallengerg, B. Svensson, J. Catal., 163 (1996) 279.

9 Y. Jiang, S. Decker, C. Mohs, K.L. Klabunde, J. Catal., 180 (1998) 24.

10 P. Larsson, A. Andersson, J. Catal., 179 (1998) 72.

11 V. Chikan, A. Monhar, K. Balazsik, J. Catal., 184 (1999) 134.

12 C.P. Poole, T. Datta, H.A. Farach, M.M. Rigney, C.R. Sanders, Copper Oxide Superconductors, John Wiley& Sons, Newyork, 1988.

13 A.S. Lanje, S.J. Sharma, R.B. Pode, R.S. Ningthoujam, Adv. in App. Sc. Res., 1 (2010) 36.

14 D. Hai-Yan, Z. Yu-Ling, L. Jing-Kui, X. Si-Shen, J. Mater. Sci., 28 (1993) 5176.

15 J. Dianzeng, Y. Jianqun, X. Xi, Chin. Sci. Bull., 43 (1998) 571.

16 C.L. Carnes, J. Stipp, K.J. Klabunde, J. Bonevich, Langmuir, 18 (2002) 1352.

17 D.K. Singh, D.K. Pandey, R.R. Yadav, Ultrasonics, 49 (2009) 634.

18 J. Hemalatha, T. Prabhakaran , R. Pratibha Nalini, Microfluid Nanofluid, 10 (2011) 263.

J. Pure Appl. Ultrason. 34 (2012) pp. 76-81

Intensification of the Chemical Degradation of Reactive Red 141 in the presence of ultrasound and Rare Earths [Lanthanum and Praseodymium]

Pankaj and Shikha Goyal
Department of Chemistry, Dayalbagh Educational Institute, Agra 282 005, INDIA.
E-mail:-pankaj2@bsnl.in

Degradation of an azo dye, Reactive Red 141 ($C_{52}H_{26}C_{12}N_{14}Na_8O_{26}S_8$) in the aqueous solution has been carried out with ultrasound (US) and in combination with rare earth ions (La^{3+} and Pr^{3+}). Both horn and tank type of sonicating devices, operating at 20 kHz and 250 W, were used for the degradation. A comparative study of continuous and pulsed mode of ultrasound induction has also been undertaken. Operational parameter, such as, initial dye concentration, pH and the presence of rare earth ions on the degradation of dye have been found to affect the degradation process . The degradation rate increased with increasing rare earth concentration, decreasing pH and initial dye concentration. The kinetic data fitted well with pseudo-first order kinetic model. The rate constant for the degradation process with US+RE was three times compared to US alone. The efficiency of various processes for the degradation of RR 141 dye was found to be in the order: US+La > US+Pr > US.

Keywords: Degradation, Ultrasound, RR 141, Rare Earth ions, Kinetics.

Introduction

Wastewater from the textile industry contained large amount of azo dyes which owing to their toxicity and carcinogenic nature was a major threat to the ecosystem[1]. Amongst the dyestuff, reactive dyes constitute a significant portion of dye pollutants. Several physical[2-4], chemical[5-7] and biological[8-10] methods are available for the treatment of textile waste water, but all these are associated with the generation of secondary pollution products, besides also required considerable amount of time and energy for their mineralisation. Therefore a green method, which may not only mineralise the dye but also required minimum time and energy, is obligatory.

The advanced oxidation processes (AOPs) involving sonolytic process[11] is based on the generation of highly reactive hydroxyl radicals[12]. These are produced due to the cavitational effect of ultrasound[13] and have been reported to degrade a variety of dyes in the presence of strong oxidising agent without the generation of secondary wastes. In terms of convenience and simplicity of operation, ultrasound has been found to be more competitive and far superior to many alternative approaches. Sonochemical treatment typically operates at ambient conditions and does not require the addition of extra chemicals or catalysts[14]. However, the ultrasonic irradiation alone has not been able to provide high enough rate of degradation. Therefore, the addition of rare earth ions, in trace quantities, has been tried and found to be potential route to enhance the decomposition efficiency and reduce the time required for the pollutant removal. The main objective of this study is to investigate the application of low frequency ultrasound alone and in combination with rare earth ions in the degradation of Reactive Red 141 dye. The effects of operating parameters such as pH, initial dye concentration, rare earth ion dosage on the degradation have also been studied. Besides, a comparison of the use of an ultrasonic probe and ultrasonic bath in terms of degradation efficiency has also been examined. The pulsed mode of ultrasonic induction to the effluent solution has been found to be still more effective in the dye degradation compared to the continuous mode, keeping all other parameters constant.

Experimental section

Materials

Highly pure sample of RR 141 dye (99.9%) was obtained as gift from M/s Spectrum Dyes and Chemicals, Surat, India. Lanthanum chloride ($LaCl_3.6H_2O$) and Praseodymium chloride ($PrCl_3.6H_2O$) [Both Indian Rare Earths Ltd, 99.99%] were kept under vacuum for 2 hr before use.

Ultrasonic equipments and degradation experiments

The degradation experiments were conducted in both ultrasonic bath (Vibronics, operating at a frequency of 20 kHz and 250 W and equipped with in-built piezoelectric transducer placed at the

*Life Fellow, Ultrasonics Society of India

rectangular bottom) and ultrasonic probe (Vibronics, Model P_2, operating at a fixed frequency of 20 kHz and 250 W and fixed on a titanium tip of 12 mm diameter).

Stock solution (1000 mg/L) of dye was prepared in triple distilled and deionised water. 10 mL of dye solution at different initial concentration (16-40 mg/L) was mixed with 5 mL of 20 mg/L RE^{3+} ions (La and Pr), wherever needed. The reaction mixture was sonicated for different time intervals (30, 60, 90 and 120 minutes) with continuously purging of dried air to keep the solution saturated with air and to enhance cavity formation. The degradation of dye was carried out under the following experimental conditions; US, US+Pr, US+La, and were followed through spectrophotometric determination of the concentration of the residual amounts of dye using Shimadzu UV-Vis spectrophotometer, 1601 PC , at λ_{max} = 544 nm. The data obtained in these studies were used to calculate the percentage degradation of dye by using the equation;

$$\% \text{ dye removal} = [(C_0\text{-}C_t)/C_0] \times 100 \quad (1)$$

where C_0 is the initial concentration of dye and C_t is the concentration of dye at time t.

Results and discussion

Degradation Monitoring by UV-Vis Spectra changes

The absorption peaks at 544 and 288 nm in Fig.1 were identified as the chromophore structure and benzene component respectively in the dye molecule. Spectral changes that occurred during different experimental processes at different irradiation time of dye have been shown in Fig-1 through a-c. Decrease in the absorbance at 544 nm indicated the removal of dye due to fragmentation of the azo links through the oxidative attack by OH radicals and the decrease of the absorbance at 288 nm was due to the degradation of the aromatic fragment of the dye molecule. The cavitational effect of US induced faster oxidation of the dye and the subsequent degradation of intermediates. The addition of REs (La and Pr), in the presence of US further improved the degradation (Fig.1 b-c, 544 nm). The shift in the absorption spectral peak from 544 to 522 nm is due to the formation of a complex between RE and dye molecules. The azo dye can strongly coordinate with RE through N atom of the azo bond and the hydroxyl group of naphthalene ring as shown in Fig. 2. La^{3+} was found to have better degradation efficiency than Pr^{3+}. Here the role of *f*- electrons and the subsequent stability of RE-dye complex is apparently visible.

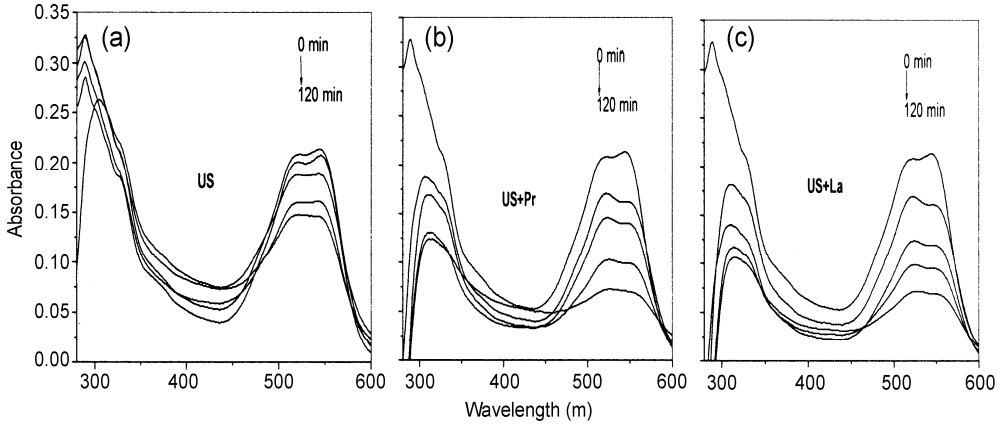

Fig. 1—UV-Vis spectra for degradation of RR 141 dye at C_0=16 mg/L, RE=20 mg/L

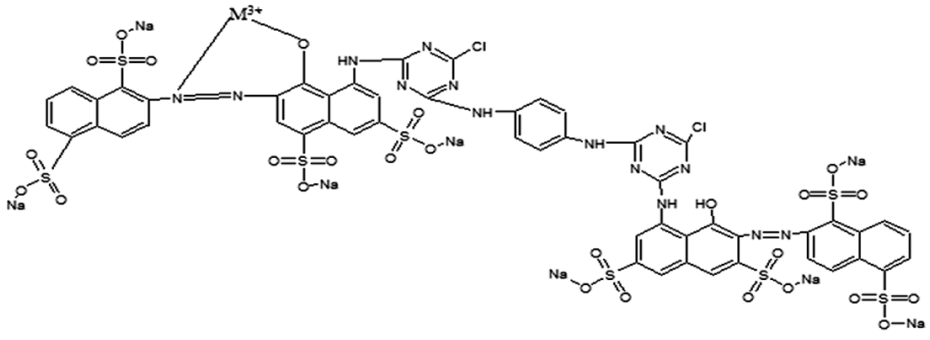

Fig. 2—Structure of Reactive Red 141 dye coordinated to metal ion

La^{3+} does not have any electron in its *f*-shell whereas the Pr^{3+} has only one $4f^1$ electron. Due to several vacant *f*- orbitals, REs are quick to form complex[15-16] by accepting and accommodating non bonding electron pair from the donor elements of the dye, but since completely vacant *f*-orbital gives extra stability to the RE ions, the complex between La^{3+} and dye is likely to be degraded faster than Pr^{3+} - dye complex, as has been found in our experiment. The degradation of Pr^{3+} - dye complex is slower due to the fact that even after the degradation of complex, Pr^{3+} ion is still left with one electron ($4f^1$) and therefore fails to achieve the most stable electronic configuration as in case of La^{3+}.

Degradation kinetics

The degradation of RR 141 dye followed pseudo first order kinetics and is given by the equation:-

$$\ln C_t = \ln C_0 - k_1 t \quad (2)$$

where C_0 is the initial concentration of dye, C_t is the dye concentration at time t and the rate constant k_1 was determined from the slope of $-\ln C_t/C_0$ vs t (Fig. 3). The time required for dye to degrade to 50% of their original value, $t_{1/2}$ was calculated from the rate constants as $0.693/k_1$[17]. Table.1 shows the rate constants and $t_{1/2}$ for degradation of dye under different conditions. Kinetic data showed that rate constants of sonodegradation reaction in the presence of rare earth ions were three times higher than US alone.

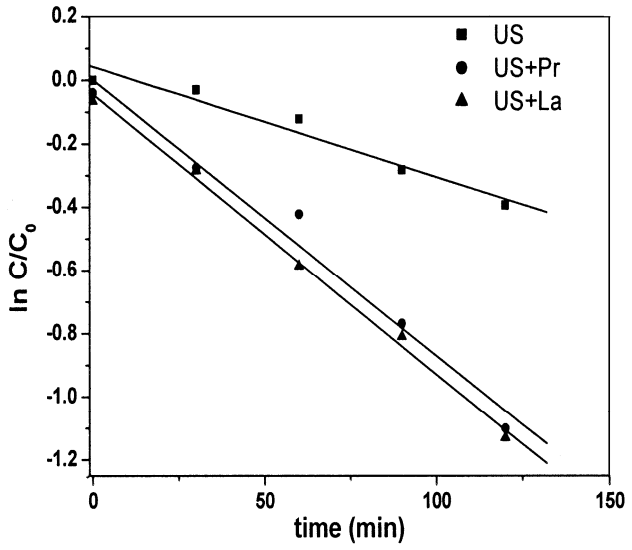

Fig. 3—Pseudo-first order kinetic plot of RR 141 under different experimental conditions at C_0=16 mg/L, RE=20 mg/L

Table.1—Half life and reaction rate constant under different experimental conditions

Parameters	Experimental conditions		
	US	US+Pr	US+La
Rate Constant (k_1) min^{-1}	0.003	0.008	0.009
Half life Time ($t_{1/2}$) min	231	86	77

Effect of initial Concentration of dye

Owing to the non-selectivity of hydroxyl radical, the competition between the dye intermediates and parent dye for hydroxyl radical becomes intense therefore, the degradation rate decreases with increase in the concentration of dye. Additionally, in the US process, the cavities approach saturation with increasing dye concentration[18]. These two factors contributed to a decreasing rate constant for the degradation of dye with an increase in initial concentration under different experimental conditions (Fig. 4).

Effect of Rare Earth ions

The effect of rare earth ions, REs, on the degradation of dye, was examined with different dye to metal ratios (4:1, 4:3 and 4:5). When dye-RE ratio was 4:1, all dye molecules were not fully coordinated to REs, hence many free sites in the dye molecules still existed. But when dye-RE ratio increased to 4:3 and 4:5 respectively, the degradation rate improved (Fig. 5) due to the saturation of all co-ordination sites of the dye. La^{3+} was, however, found to have better degradation efficiency than Pr^{3+}.

Effect of pH

Study of the pH dependence of degradation at pH values 5, 7 and 9 respectively, have been shown in Fig. 6.

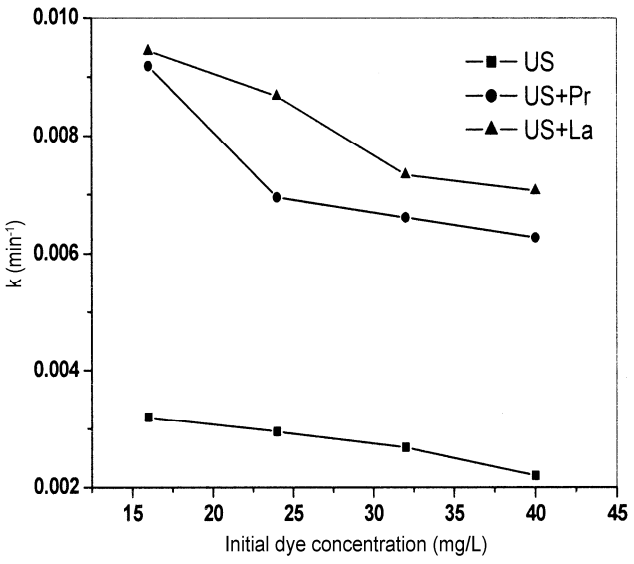

Fig. 4—Rate constants of RR 141 degradation under US, US+Pr and US+La, as a function of initial dye concentration (16-40 mg/L), RE= 20 mg/L , time = 120 min

The efficiency of RR 141 degradation increased in acidic medium, while decreased in basic conditions. The acceleration was probably associated with the effect of protonation of negatively charged $-SO_3^-$ groups in acidic medium and the hydrophobic character of the resulting molecule enhanced its reactivity under ultrasound treatment. On the contrary, under alkaline condition, the hydrogen loss from the protonated site

$(-SO_3H \rightarrow -SO_3^-;\ Ar-OH \rightarrow Ar-O^-)$ resulting in enriched hydrophilic characteristics. Moreover, under acidic pH, hydroxyl radical is the predominant reactive oxidant[19] and under alkaline pH, hydroperoxyl (HO_2) radical do not have as high oxidising power as hydroxyl radical. HO_2 is produced from the reaction of H_2O_2 with hydroxyl radicals[20]. Also, under extreme alkaline conditions, H_2O_2 scavenging effects become more significant.

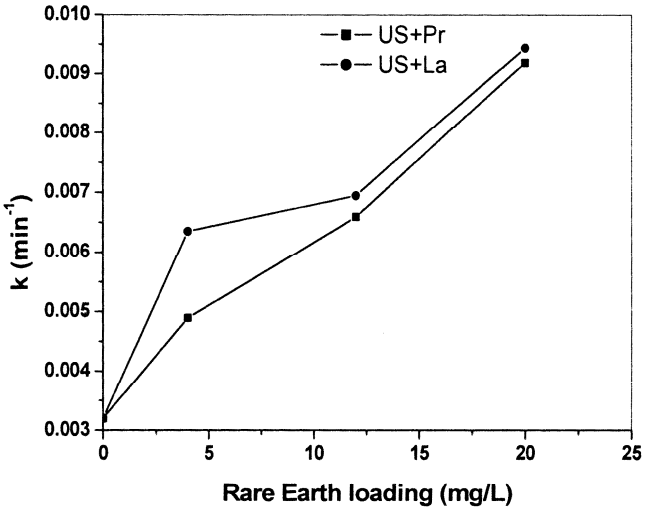

Fig. 5—Rate constants of RR 141 degradation under US+Pr and US+La, as a function of rare earth ion concentration, C_0 = 16 mg/L, time = 120 min

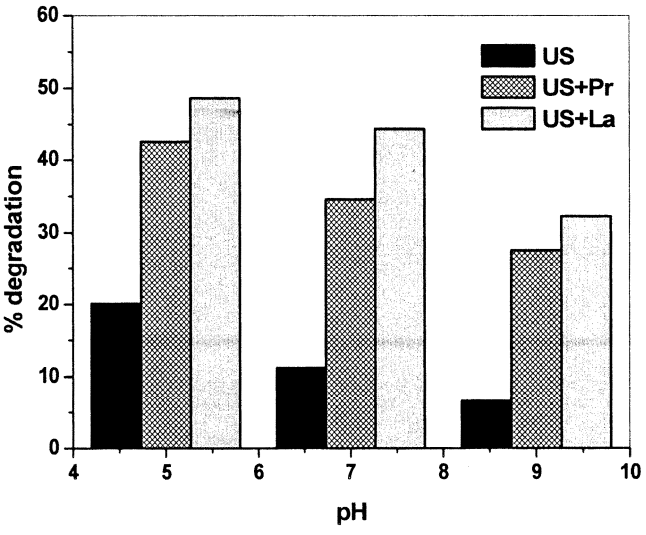

Fig. 6—Effect of pH on degradation efficiency of RR 141, C_0 = 16 mg/L, RE = 20 mg/L, time = 60 min

Effect of bath and probe type sonicator

The degradation rate was lower in case of ultrasonic bath compared to the ultrasonic processor for all time intervals (Fig.7a-c). The ultrasonic processor transmitted ultrasound directly into the

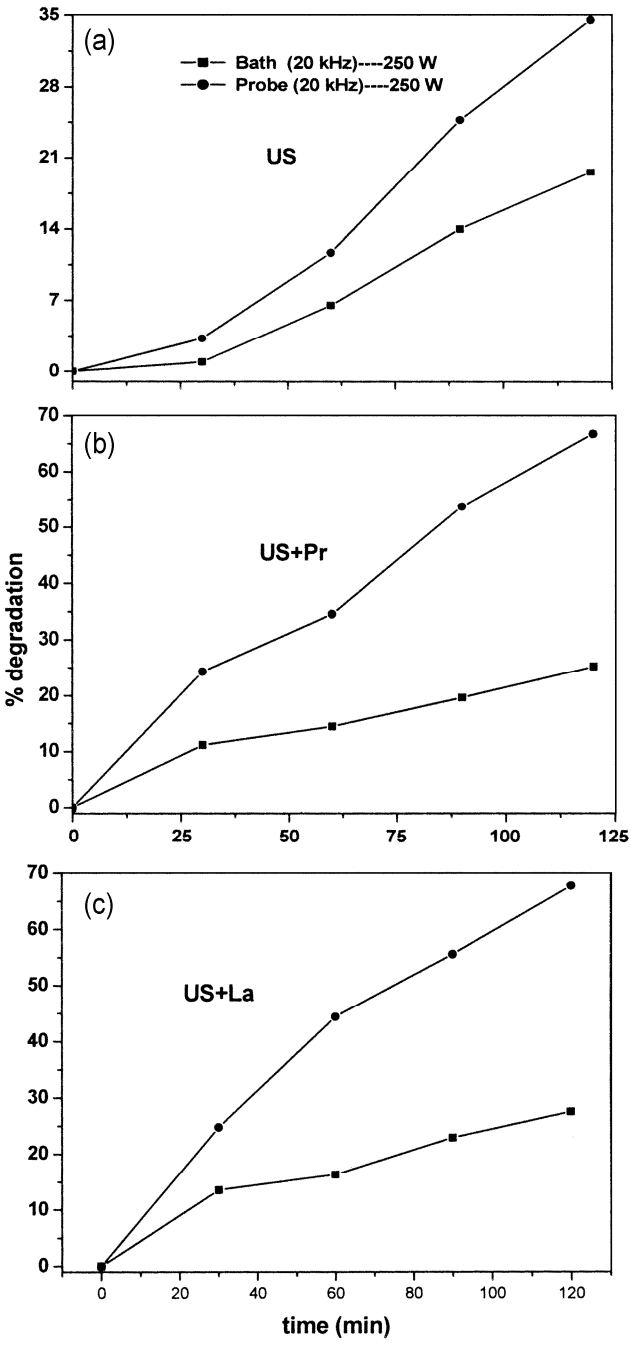

Fig. 7—Comparison between probe and bath type sonicator, C_0 =16 mg/L, RE =20 mg/L

Table. 2—Comparison between Continuous (C) and pulsed (P) mode at different initial dye concentration (C_0), time =60 min

C_0 (ppm)		% degradation		
		US	US+Pr	US+La
16	C	11.68	34.57	44.39
	P	19.15	40.19	49.53
24	C	10.81	33.78	42.97
	P	17.29	37.83	45.67
32	C	10.38	31.45	39.73
	P	15.28	34.84	41.43

reaction cell without much loss of sonic energy; whereas in the ultrasonic bath the ultrasound waves were attenuated by the fluid of the tank and the glass material of the reaction vessel, therefore failed to transfer the sufficient acoustic energy.

Effect of operation mode

To examine the efficiency of degradation on the modes of ultrasound induction, the degradation was examined through continuous (C) and pulsed (P) modes (5 min ON/5 min OFF) at different concentrations of dye. The degradation was higher in pulsed mode for all dye concentrations (Table 2). It was due to generation of cavitation bubbles with a longer lifetime in pulsed mode rather than continuous mode of ultrasound induction[21]. The longer lifetime could allow more time for relatively large, surface active molecules to accumulate[22] at the gas/solution interface of cavitational bubbles, where higher temperature and radical concentration exist and thus the degradation of dye was enhanced under pulsed ultrasound.

Conclusion

Ultrasound could degrade the dye, but when used in combination with rare earth ions, its degradability enhanced significantly. Ultrasound increased the amount of reactive radical species such as singlet oxygen, superoxide and hydroxyl radicals inducing oxidation of the dye. The degradation of dye followed pseudo-first order kinetics. The degradation rate increased with increase in rare earth amount while the rate decreased with increase in initial concentration of dye and the pH of the solution. Ultrasonic probe gave better degradation rate as compared to ultrasonic bath. Results further indicated that the pulsed mode of ultrasound induction improved the efficiency of ultrasonic degradation through the accumulation of dye molecules at the gas/solution interface of cavitation bubbles.

Acknowledgement

Authors acknowledge DAE–BRNS for the financial support and SG is grateful to CSIR for JRF.

References

1 Li, J.T., Bai, B. and Song, Y.L., Degradation of acid orange 3 in aqueous solution by combination of Fly ash/H_2O_2 and ultrasound irradiation, *Indian J. Chem. Technol.*, 17 (2010) 198-203.

2 Meric, S., Selcuk, H. and Belgiorno, V., Acute toxicity removal in textile finishing waste water by Fenton's oxidation, ozone and coagulation-flocculation processes, *Water Res.*, 39 (2005) 1147-1153.

3 Ledakowicz, J.S., Koprowski, T., Machnowski, W. and Khudsen, H. H., Membrane filtration of textile dye house waste water for technological water reuse, *Desalination*, 119 (1998) 1-9.

4 Laszlo, J.A., Regeneration of azo dyes-saturated cellulosic anion exchange resin by burkholderia cepacia anaerobic dye reduction, *Environ.Sci.Technol.*, 34 (2000) 167-172.

5 Ian,B. and Peters, A.T., Photochemical degradation of aminoazobenzene disperse dyes in ethanolic solution:part i: effect of concentration, water, and temperature, *Text.Res.J.*, 44 (1974) 639.

6 Wang, X., Jia, J. and Wang, Y., Electrochemical degradation of reactive dye in the presence of water jet cavitation, *Ultrason.Sonochem.,*17 (2010) 515-520.

7 Kuo, W.S. and Ho, P.H., Solar photocatalytic decolorization of methylene blue in water, *Chemosphere*, 45 (2001) 77-83.

8 Capalash,N. and Sharma, P., Biodegradation of textile azo dyes by phanerochaete chrysoporium, *world J. Microbiol. Biotechnol.,* 8 (1992) 309-312.

9 Sharma, D.K., Saini, H.S., Singh, M., Chimni, S.S. and Chadha, B.S., Biological treatment of textile dye acid violet-17 by bacterial consortium in an up-flow immobilized all bioreactor, *Lett Appl Microbiol.*, 38 (2004) 345-350.

10 Palamthodi, S., Patil, D. and Patil, Y., Microbial degradation of textile industrial effluents, *Afr.J.Biotechnol.,* 10 (2011) 12687-12691.

11 Tezcanil, G.G. and Ince, N.H., Degradation and toxicity reduction of Textile dyestuffs by ultrasound, *Ultrasonics Sonochem.*, 10 (2003) 235-240.

12 Ozen,A.S., Aviyente, V., Proft, F.D. and Geerlings, P., Modelling the substituent effect on the oxidative degradation of azo dyes *J. Phys. Chem. A.,* 108 (2004) 5990-6000.

13 Mason ,T.J., Ultrasound in synthetic organic chemistry, *Chem. Soc. Rev.,* 26 (1997) 443-451.

14 Kritikos, D.E., Xekoukoulotakin, N.P., Psillakis, E. and Mantzavinos, D., Photocatalytic degradation of reactive black 5 in aqueous ssolutions : Effect of operating conditions and coupling with ultrasound, *Water Res.,* 41 (2007) 2236-2246.

15 Liang, C.H., Li, F.B., Liu, C.S., Lu, J.L. and Wang, X.G., The enhancement of adsorption and photocatalytic activity of rare earth ions doped TiO_2 for the degradation of orange I, *Dyes Pigm.*,76 (2008) 477-484.

16 Shi, J.W., Zheng, J.T. and Wu, P., Preparation, characterization and photocatalytic activities of holium-doped titanium dioxide nanoparticles, *J.Hazard. Mater.*, 161 (2009) 416-422.

17 Guivarch, E., Trevin, S., Lahitte, C. and Oturan, M.A., Degradation of azo dyes in water by Electro-Fenton process, *Environ Chem Lett.*, 1 (2003) 38-44.

18 Lucas, M.S. and Peres, J.A., Decolorization of the azo dye reactive black 5 by fenton and Photo-fenton oxidation, *Dyes Pigm.*, 71 (2006) 236-244.

19 Vajnhandl, S. and Marechal, A.M.L., Case study of the sonochemical decolouration of textile azo dye reactive black 5, *J.Hazard. Mater.*, 141 (2007) 329-335.

20 Vajnhandl, S. and Marechal, A.M.L., Ultrasound in textile dyeing and the decolouration/mineralisation of textile dyes, *Dyes Pigm.*, 65 (2005) 89-101.

21 Yang, L., Sostaric, J.Z., Rathman, J.F., Kuppusamy, P. and Weavers, L.K., effects of pulsed ultrasound on the adsorption of n-alkyl anionic surfactants at the gas/solution interface of cavitation bubbles, *J.Phys.Chem.B.*, 111 (2007) 1361-1367.

22 Yang, L., Sostaric, J.Z., Rathman, and Weavers, L.K., effect of ultrasound frequency on pulsed sonolytic degradation of octylbenzene sulfonic acid, *J.Phys.Chem.B.*, 112 (2008) 852-858.

J. Pure Appl. Ultrason. 34 (2012) pp. 82-85

Theoretical Prediction of Ultrasonic velocity through Collision Factor Theory in Binary Liquid Mixtures at 308.15K

Tanuja Nautiya[la] and J. D. Pandey[b]*

[a]Department of Applied Chemistry, Northern India Engineering College, Guru Gobind Singh Indraprastha University, New Delhi

[b]Department of Chemistry, University of Allahabad, Allahabad
E-mail : tanujanautiyal@yahoo.co.in

Ultrasonic velocity has been a subject of active interest during the recent past. Sound velocity is highly useful in understanding the molecular interactions in binary and ternary liquid mixtures. Attempts have been made to show the significance of thermodynamic properties derived from sound velocity and related data. Collision Factor theory, in which molecules of liquids have been taken as a real non-elastic substance, sound velocity is directly related to molecular radii. Four different relations have been used for determining theoretical sound velocity and then compared with experimental sound velocity to check the validity of all four relations.

Keywords: Collision factor theory, sound velocity, molecular radii.

1. Introduction

Ultrasonic velocity[1-4] of a liquid is related to the binding forces between the atoms or the molecules. Measurement of ultrasonic velocity gives information about physico-chemical behavior of solutions and liquid mixtures and molecular interactions of multi-component liquid mixtures. In Collision Factor Theory[5], molecules are treated as real, non-elastic molecules. The study of the solution properties of liquid mixtures consisting of polar as well as non - polar components finds applications in industrial and technological processes. Those binary mixtures, in which both components are polar organic liquids, they have strong interaction. Hence their collisions are likely to be elastic, resulting in greater extent of interaction.On the basis of collision factor theory Schaff gave the following relation for ultrasonic velocity;

$$u = \left\{ u_\infty S\left[\frac{B}{V}\right]\right\} \quad \ldots (1)$$

where u_∞ = 1600ms^{-1}, S = collision factor and B = actual molecular volume per mole

$$B = \left\{ \tfrac{4}{3}\pi r_m{}^3 N \right\} \quad \ldots (2)$$

Here r_m stands for molecular radius and N for Avagadro number. For the computation of B, we have taken four different relations given by Schaff *et al*[6], Gopala Rao *et al*[7], Eyring *et al*[8] and kittel *et al*[9]. The relation between molecular radius and other physical parameters of the liquid is based on the Vander Waals equation.

$$r_m(Schaff) = \sqrt[3]{\frac{M}{\rho N}}\left\{\sqrt[3]{\frac{3}{16\pi}\left[1-\frac{\gamma RT}{Mu^2}\right]\left(1+\frac{Mu^2}{3\gamma RT}-1\right)}\right\} \quad \ldots (3)$$

$$r_m(Rao) = \sqrt[3]{\frac{M}{\rho N}}\left\{\sqrt[3]{\frac{3}{16\pi}\left[1-\frac{\gamma RT}{Mu^2}\right]\left(1+\frac{Mu^2}{\gamma RT}-1\right)}\right\} \quad \ldots (4)$$

Eyring and kittel's methods are based on the assumption that the macroscopic velocity of sound results from two processes: the propagation of sound waves inside the molecules, the velocity of which is assumed to be infinite and through the free space between them.

$$r_m(Kittel) = \sqrt[3]{\frac{M}{\rho N}\frac{1}{2}\left\{\sqrt[3]{1-\left[1-\frac{1}{u}\sqrt{\frac{3\gamma RT}{M}}\right]^3\sqrt{2}}\right\}} \quad \ldots (5)$$

$$r_m(Eyring) = \sqrt[3]{\frac{M}{\rho N}\frac{1}{2}\left\{\sqrt[3]{1-\left[1-\frac{1}{u}\sqrt{\frac{\gamma RT}{M}}\right]^3\sqrt{2}}\right\}} \quad \ldots (6)$$

Here M is the molecular weight,ρ is the density, γ is the specific heat ratio (β_T\ β_S), T is the temperature in Kelvin, u is the velocity of sound in the liquid under test, N is the Avagadro number.

This concept of CFT is applied for binary liquid mixtures by Nutch-Kuhunies[10] for calculating the

*Life fellow : Ultrasonics Socieiy of India

ultrasonic velocity in binary liquid mixtures using the relation

$$u_{mix} = u_{\infty}\left(x_1 S_1 + x_2 S_2\right).\left(\frac{x_1 B_1 + x_2 B_2}{V_m}\right) \quad \ldots (7)$$

In order to check how the molecular radius affects the ultrasonic velocity, we have made four sets of equation by four different equations of molecular radii and later these values are utilized in eq.1 for theoretical sound velocity. In the present investigation, the ultrasonic velocity of binary liquid mixtures methyl propanoate (x_1) + n-heptane, methyl propanoate (x_1) + benzene, methyl propanoate (x_1) + chlorobenzene and methyl propanoate (x_1) + 1,1,2,2. tetrachloroethane have been theoretically evaluated by using four different equations of molecular radius and these theoretical values are compared with experimental values[11].

Molecular parameters of pure liquids are reported in Table 1 and Theoretical ultrasonic velocities of four different binary liquid mixtures have computed by using four different equations and compared with experimental data are recorded in Table 2.

The standard deviations for binary liquid mixtures by four different equations are recorded in Table 3

2. Result & discussion

As mentioned above that, Rao's equation differs from that of Schaff's only by the lack of coefficient 1/3 in the second term of the expression, $u = \left\{1 + .\left[\frac{Mu^2}{3\gamma RT}\right]\right\}^{1/2}$, so for all the liquids and liquid mixtures, the value of radii obtained by the Rao's method are ~3% lower than those calculated by Schaff's method. Therefore, it is evident from Table 2, where we get nearly 3% less deviation by Rao's methods. Close perusals of systems; methyl propanoate + n-heptane, methyl propanoate + benzene, methyl propanoate + chlorobenzene, methyl propanoate + 1,1,2,2. tetrachloroethane, shows that standard percentage deviation ranges from 0.00 to 2.44. Theoretical sound velocity computed by using equations of Schaff, Rao, Kittel give fair agreement with the experimental value of sound velocity and maximum deviation is obtained by Eyring's method. Best results have been obtained in binary solutions of methyl propanoate (x_1) + chlorobenzene and methyl propanoate (x_1) + 1,1,2,2. tetrachloroethane.

From the behavior of above mentioned liquid solutions, under the present investigation, it can be

Table 1—Molecular parameters of pure liquids at 308.15K

Liquids	Viscosity (mPas)	ultrasonic velocity (ms^{-1})	isothermal expansion coefficient (kK^{-1})	molar heat capacity ($Jdeg^{-1}mol^{-1}$)
n-heptane	0.353	1095.0	1.277	228.6
Benzene	0.537	1255.0	1.244	137.1
Chlorobenzene	0.675	1224.0	1.057	151.4
1,1,2,2 tetrachloroethane	1.406	1124.0	0.658	166.3
methylpropanoate	0.437	1130.0	0.769	175.9

Table 2—Theoretical sound velocity and experimental sound velocity for four binary liquid mixture

Methylpropanoate (x_1)+ n-heptane (x_2):

x_1	u(Exp) (ms^{-1})	u(Eq.3) (ms^{-1})	u(Eq.4) (ms^{-1})	u(Eq.5) (ms^{-1})	u(Eq.6) (ms^{-1})
0.0447	1091.0	1087.1	1072.7	1094.9	1232.6
0.1083	1086.0	1089.0	1074.0	1094.9	1241.4
0.1932	1081.0	1091.0	1076.0	1092.5	1251.4
0.3018	1076.0	1095.0	1078.9	1091.3	1262.6
0.4146	1075.0	1098.0	1082.6	1078.1	1270.2
0.5227	1077.0	1102.6	1086.6	1084.2	1274.2
0.5693	1076.0	1104.2	1088.2	1088.3	1276.5
0.7002	1083.0	1109.3	1094.2	1092.3	1274.5
0.7986	1093.0	1113.5	1099.5	1098.2	1267.4
0.9016	1109.0	1118.2	1106.1	1109.5	1253.5
0.9509	1118.0	1120.6	1109.5	1118.5	1244.9

(*Contd.*)

Table 2—Theoretical sound velocity and experimental sound velocity for four binary liquid mixture (*Contd*.)

Methylpropanoate (x_1) + Chlorobenzene (x_2):

x_1	u(Exp) (ms^{-1})	u(Eq.3) (ms^{-1})	u(Eq.4) (ms^{-1})	u(Eq.5) (ms^{-1})	u(Eq.6) (ms^{-1})
0.0485	1224.0	1219.5	1219.9	1219.3	1218.2
0.0993	1223.0	1214.6	1214.7	1212.5	1216.1
0.2038	1217.0	1204.3	1203.7	1201.9	1214.5
0.2614	1212.0	1198.5	1197.4	1196.9	1214.8
0.4087	1196.0	1183.5	1180.9	1185.8	1218.2
0.4556	1191.0	1178.8	1175.6	1181.5	1219.2
0.6041	1177.0	1163.8	1159.1	1167.4	1221.0
0.7011	1167.0	1153.9	1148.2	1159.3	1222.6
0.8064	1155.0	1143.2	1136.2	1150.8	1225.2
0.9054	1144.0	1133.1	1124.8	1139.8	1227.8
0.9486	1138.0	1128.6	1119.7	1134.7	1230.0

Methylpropanoate (x_1) + benzene (x_2):

x_1	u(Exp) (ms^{-1})	u(Eq.3) (ms^{-1})	u(Eq.4) (ms^{-1})	u(Eq.5) (ms^{-1})	u(Eq.6) (ms^{-1})
0.0415	1251.0	1249.8	1249.9	1244.6	1250.8
0.1037	1246.0	1241.6	1241.3	1226.3	1248.3
0.2041	1234.0	1228.3	1226.9	1203.9	1246.6
0.3026	1225.0	1215.5	1213.3	1183.9	1242.6
0.4053	1213.0	1202.0	1198.7	1168.8	1240.0
0.4569	1206.0	1195.1	1191.3	1162.9	1239.3
0.6013	1187.0	1176.0	1170.7	1146.8	1237.2
0.7026	1173.0	1162.6	1156.2	1139.4	1235.9
0.8018	1159.0	1149.5	1142.0	1135.2	1234.6
0.9039	1144.0	1135.9	1127.3	1131.8	1234.0
0.9674	1135.0	1127.5	1118.2	1130.7	1233.2

Methylpropanoate (x_1) + 1,1,2,2,tetrachloroethane (x_2):

x_1	u(Exp) (ms^{-1})	u(Eq.3) (ms^{-1})	u(Eq.4) (ms^{-1})	u(Eq.5) (ms^{-1})	u(Eq.6) (ms^{-1})
0.0501	1132.0	1125.2	1126.5	1125.0	1111.9
0.1021	1136.0	1125.7	1127.4	1129.4	1111.2
0.2031	1134.0	1126.2	1127.9	1134.8	1119.2
0.3020	1128.0	1126.3	1127.4	1136.1	1132.2
0.3398	1125.0	1126.1	1127.1	1138.4	1137.7
0.5038	1117.0	1126.0	1125.4	1142.0	1160.8
0.6012	1115.0	1125.8	1124.0	1142.5	1174.2
0.6946	1116.0	1125.5	1122.3	1140.1	1186.6
0.7988	1118.0	1124.9	1119.9	1137.3	1201.9
0.9016	1125.0	1124.2	1117.2	1132.8	1215.6
0.9481	1123.0	1123.6	1115.1	1140.1	1226.1

Table 3—Standard deviation from experimental value for all four binary liquid mixtures

Liquid Mixtures	u (Eq.3)	u (Eq.4)	u (Eq.5)	u (Eq.6)
1. Methylpropanoate (x_1)+ n-heptane (x_2):	0.096	0.000	0.027	2.442
2. Methylpropanoate (x_1) + Chlorobenzene (x_2):	0.044	0.080	0.026	0.455
3. Methylpropanoate (x_1) + benzene (x_2):	0.023	0.056	0.255	0.669
4. Methylpropanoate (x_1) +1,1,2,2,tetrachloroethane (x_2):	0.000	0.000	0.056	0.552

said that the positive deviations in velocity are attributed to (a) molecular association and (b) complex formation. Negative deviations in velocity are attributed to the molecular dissociation of an associated species caused by addition of an inert solvent or an active solvent. The actual sign and magnitude of the deviations depend upon the relative strength of the two opposite effects (molecular association and dissociation). In Collision Factor Theory, molecules are treated as real, non-elastic molecules. Binary liquid mixtures, methyl propanoate (x_1) + chlorobenzene and methyl propanoate (x_1) + 1,1,2,2. tetrachloroethane, in which both components are polar organic liquids, these have strong interaction. Hence their collisions are likely to be elastic, resulting in greater extent of interaction. The reason behind this can be attributed to the presence of two empirical factors S_1 and S_2, contained in equation (7), which are known as collision factors and are in fact correction terms which can be adjusted to give better results. As mentioned above, interactions are results of active collisions between the molecules. For binary liquid mixtures (polar + polar), Schaff's relation seems to provide the best results.

Conclusion

From the above results, we conclude that ultrasonic velocities predicted by Collision Factor Theory, by using four equations for calculating molecular radii were compared with experimentally measured velocity values at 308.15K in the two component mixtures. Among the four theories, it is found that the Schaff's method is most reliable method to obtain molecular radius.

References

1 Ultrasonic Velocity, density, viscosity and their excess parametes of the binary mixtures of THF with Methanol and o-cresol at varying temperatures., Parveen S, Shukla Divya,Singh Shashi, Singh K P, Gupta Manisha & Shukla J P, *Applied Acoustics*, 70 (3), (2009), 507-513.

2 Excess molar volumes of *N*,*N*-dimethylformamide+2-pentanone+alkan-1-ols mixed solvent systems at 303.15K.., Venkatesu P, Chandrashekhar G, Prabhakar Rao M. V & Tadensz Hofman, *Thermodynamica Acta,* 443 (2006), 62.

3 Ultrasonic and Theoretical studies of some ternary liquid mixtures at various temperatures., Sumanthi T & Uma Maheshwari J, *Ind Jou of Pure & Applied Physics*, vol 47, (2009), 782-786.

4 Ultrasonic studies of liquid mixtures., Pandey J D & Shukla A K, *J.Pure Appl. Ultrason,* 15 (1993) 37.

5 Schaff W, *Moleklara Bustik, Springer Verlag,* Berlin (1963) Chap XI & XII.

6 Schaff W, *Acustica,* 33 (1975) 587.

7 Gopala Rao R V & Venkataseshaiah, *Z Phys Chem,* 242 (1969) 193.

8 Free Volumes and Free Angle Ratios of Molecules in Liquids., Kincaid J F & Eyring H, *J Chem Phys,* 6 (1938), 620.

9 Ultrasonic Propagation in Liquids. II. Theoretical Study of the Free Volume Model of the Liquid State., Kittel Ch, *J Chem Phys,* 14 (1946) 614.

10 Nutsch- Kuhnkies, *Acustica,* 15 (1965), 383.

11 Viscosities, speeds of sound and excess isentropic compressibilities of binary mixtures of alkyl alkanoate–hydrocarbons at 308.15 K and 318.15 K., Sastry N V, Jain N J , George A & Bahadur P, *Fluid Phase Equillib,* 163 (1999), 275.

J. Pure Appl. Ultrason. 34 (2012) pp. 86-89

Effect of temperature on ultrasonic speed and related acoustical parameters of cardo polysulfonate of bisphenol-A and 4, 4'-disulfonyl chloride diphenyl ether solutions

S. K. Matariya and P. H. Parsania*

Department of Chemistry, Polymer Chemistry Division,
Saurashtra University, Rajkot- 360 005, India
*Email: phparsania@aol.com and phparsania22@gmail.com

The density (ρ), viscosity (η) and ultrasonic speeed (U) (2 MHz) of pure solvents: 1,2-dichloro ethane, chloroform, THF and 1,4-dioxane and copolysulfonate (PSAE) solutions have been investigated at 303, 308 and 313^{0}K. Various acoustical parameters such as specific acoustical impedance (Z), isentropic compressibility (κ_a), Rao's molar sound function(R), Van der Waals constant(b), internal pressure(π), free volume (V_f), intermolecular free path length (L_f), classical absorption coefficient $(\alpha/f^2)_{cl}$ and viscous relaxation time(τ) have been determined from ρ, η and U data and correlated with concentration at temperature. A fairly good to excellent correlation between a given parameter and concentration is observed at all temperatures and solvent systems studied. Increase or decrease of acoustical parameters with concentration and temperature indicated existence of strong molecular interactions. The effect of temperature, concentration and solvent on acoustical properties is discussed. The positive values of solvation number (S_n) suggested structure forming tendency of the polymer.

Keywords Ultrasonic velocity; density; viscosity; acoustical parameters; solvation number; molecular interactions

Introduction

An extensive use of polymer processing from solutions has necessitated investigation of molecular interactions. Acoustical properties of solutions furnish a wealth of information on molecular interactions occurring in the solutions to understand structure of polymers and also furnish knowledge on solvophilic or solvophobic nature of polymers and the strength of interactions[1,2]. Ultrasonic testing and evaluation techniques are widely used in dentistry, biochemistry, engineering, consumer and process industries, etc.[3,4] Ultrasonic technique is proved to be a powerful and effective tool for the investigation of properties of polymer solutions and behavior of polymer chains in an ultrasonic field[1,4]. It offers a rapid nondestructive method for characterizing materials.

A considerable work on ultrasonic studies of aromatic cardo polysulfonates solutions has been reported from this laboratory[5-15] To the best of our knowledge no work has been reported on ultrasonic study of poly(2,2'-propylidene-4,4'-diphenylenediphenylether-4,4'-disulfonate) (Scheme1), which prompted us to investigate molecular interactions occurring in solutions with the aid of various acoustical parameters.

Experimental Materials

The laboratory grade solvents and chemicals were purified by appropriate treatment[16] prior to their use in this work. PSAE, used in present investigation was synthesized by interfacial polycondensation technique and was purified three times from chloroform-n-hexane system ([η] = 0.57 dlg^{-1} in chloroform at 35°C).

Characterization

The density (ρ), viscosity (η) and ultrasonic speed (U) measurements of pure solvents (chloroform, 1,2-dichloroethane, 1,4-dioxane and tetrahydrofuran) and solutions were carried out at 303, 308, and 313°K by using specific gravity bottle, Ubbelohde suspended level viscometer and ultrasonic interferometer operating at 2 MHz, respectively. The ρ, η and U measurements were accurate to ±0.0001 gcm^{-3}, ±0.01 mPas and ±0.84 ms^{-1}, respectively.

Results and Discussion

The ρ, η and U data of pure solvents and solutions at 303, 308, and 313 °K are reported in Table 1. The observed trends of these data are as follow: For ρ: CF > DCE > DO >THF; for η: DO > DCE > CF >THF; and for U: DO > THF >DCE > CF. The ρ, η and U

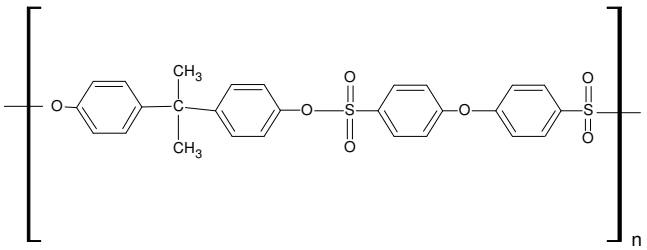

Scheme 1 Poly (2,2'-propylidene-4,4'- diphenylene diphenyl ether-4,4'-disulfonate) (PSAE)

*Life member, Ultrasonic Society of India

Table 1—Density (ρ), viscosity (η) and ultrasonic speed (U) data of PSAE solutions at different temperatures

Conc., mol/ lit	Density (ρ,kg / m^3)			Viscosity (η. 10^3, Pas)			U, (ms^{-1})		
	303 K	308 K	313 K	303 K	308 K	313 K	303 K	308 K	313 K
				PSAE + CF					
0	1.4609	1.4535	1.4427	0.5679	0.5297	0.5144	2.4060	2.3770	2.3440
0.5	1.4525	1.446	1.4346	0.6308	0.5947	0.5859	2.4040	2.3650	2.3430
1.0	1.4504	1.4443	1.4324	0.7430	0.7127	0.6613	2.4070	2.3730	2.3480
2.0	1.4491	1.4417	1.431	0.9232	0.8647	0.7865	2.4160	2.3920	2.3550
3.0	1.4479	1.4409	1.4298	1.1150	1.0395	0.9669	2.4240	2.4030	2.3630
4.0	1.4465	1.4394	1.428	1.3133	1.2233	1.1558	2.4370	2.4080	2.3670
				PSAE + DCE					
0	1.2479	1.235	1.233	0.7619	0.7162	0.7075	2.9250	2.8740	2.8330
0.5	1.2496	1.2365	1.2352	0.8985	0.8541	0.8426	2.9350	2.8830	2.8460
1.0	1.2507	1.2377	1.2364	1.0849	1.0261	1.0035	2.9430	2.8930	2.8550
2.0	1.2523	1.2395	1.2383	1.3776	1.3049	1.2909	2.9520	2.9020	2.8650
3.0	1.254	1.2412	1.2403	1.7769	1.6644	1.6501	2.9580	2.9070	2.8750
4.0	1.2557	1.2432	1.2424	2.2615	2.1372	2.1128	2.9630	2.9170	2.8830
				PSAE + DO					
0	1.0254	1.0196	1.0131	1.1112	1.0529	1.0282	3.3030	3.2470	3.1970
0.5	1.026	1.0202	1.0138	1.2063	1.1300	1.0967	3.2910	3.2470	3.1960
1.0	1.0277	1.0219	1.0156	1.2199	1.2189	1.2033	3.2970	3.2530	3.2070
2.0	1.0296	1.0235	1.0173	1.5623	1.4668	1.4246	3.3030	3.2580	3.2120
3.0	1.0315	1.0256	1.0194	1.9257	1.8219	1.7760	3.3070	3.2620	3.2250
4.0	1.034	1.0281	1.0211	2.4472	2.3032	2.2369	3.3140	3.2670	3.2330
				PSAE + THF					
0	0.8689	0.8529	0.8463	0.4682	0.4144	0.3774	3.1320	3.0860	3.0510
0.5	0.8709	0.8542	0.8482	0.5596	0.5125	0.4731	3.1220	3.0740	3.0340
1.0	0.8742	0.8575	0.8511	0.6811	0.6243	0.5867	3.1270	3.0810	3.0370
2.0	0.8774	0.8609	0.8545	0.8574	0.7744	0.7129	3.1320	3.0850	3.0390
3.0	0.8806	0.8652	0.8586	1.1415	1.0205	0.9443	3.1340	3.0920	3.0420
4.0	0.8855	0.8693	0.8626	1.4810	1.3556	1.2600	3.1360	3.0960	3.0480

increased linearly with concentration (C) and decreased linearly with temperature (T) in all the solvent systems studied. Fairly good to excellent correlationships are observed in the studied systems indicating presence of strong molecular interactions occurring in the solutions. The observed regression coefficients are 0.948-0.999, 0.969-0.999 and 0.904-0.987, respectively for ρ, η and U data. Such linear behavior is also observed in other polysulfonates solutions[5-15].

The change in ρ and U with C and T are not as appreciable as η because molecular motion is much more affected by polymer-solvent and polymer-polymer interactions in solutions[17-21]. Increase in ρ, η and U with C supported increase in cohesive forces due to powerful molecular interactions, while decrease of these parameters with T indicated decrease in cohesive forces. The increasing temperature shows increase of molecular interactions (structure formatting tendency) and destruction of structure formed previously as a result of thermal fluctuations[22]. The density and viscosity of medium, pressure, temperature, etc. affect the velocity. The molecular interactions cause chain expansion and hence increase in viscosity. A polymer-solvent interaction in solutions is of great value since the extension of chain is markedly influenced by the molecular interactions, which furnish knowledge on solvophilic or solvophobic nature of the polymers. The solvated molecules affect polymer processing from solutions.

Various acoustical parameters namely specific acoustical impedance (Z), adiabatic compressibility (κ_a), Rao's molar sound function (R), Van der Waals constant (b), internal pressure (π), free volume (V_f), intermolecular free path length (L_f), classical absorption coefficient $(\alpha/f^2)_{cl}$ and viscous relaxation time (τ) were derived by using standard equations mentioned in the literature[20].

The linear increase in Z, R, π, b, $(\alpha/f^2)_{cl}$ and τ (R^2 = 0.998-0.975) with increasing C and linear decrease with increasing T; and similarly linear decrease in κ_s, L_f and V_f (R^2 = 0.989-0.955) with increasing C and linear increase with increasing T

supported existence of powerful molecular interactions in the solutions. Thus, fairly good to excellent correlation is observed between said parameters with concentration. Practically very small temperature effect is observed in case of R, while considerable temperature effect is observed in case of b, π, V_f, $(\alpha/f^2)_{cl}$ and τ but pronounced concentration and temperature effect is observed in rest of the cases, i.e. U, Z, κ_s and L_f. Molecular interactions (solvent-solute, solute-solute and solvent-solvent) are governed by many factors namely concentration, temperature, pressure, viscosity and density of the medium, nature of the solvents and solutes, nature of substituents, etc. Powerful molecular interactions lead to increase in cohesive forces and hence either increase or decrease of a particular acoustical property. Increasing concentration leads to solute-solute interactions, which interfere the solvent-solute interactions and overall effect will be nonlinear after certain critical concentration. Generally increasing concentration and temperature both favor increase in molecular interactions, which are mainly governed by the nature of solvents and solutes and their structures. Linear increase or decrease of any acoustical properties with C and T confirms that solvent-solute interactions are powerful over those of solute-solute interactions. Such behavior is also observed in other polysulfonates having different main chain structures and substituents[5-15]. When solute-solute interactions come in picture, under such circumstances observed change will be nonlinear. Above facts are dependent on various factors as mentioned previously.

Sulfonate and ether linkages in polysulfonate molecule are more electronegative parts, which undergo H-bond formation with H-atom of chloroform, while lone pairs of electrons of 1,4-dioxane and THF, and Cl-atoms of chloroform and 1,2-dichloroethane are more electronegative parts disfavoring molecular association with the said groups of the polymer but they may favor interactions with isopropyl and aromatic linkages. Observed change in acoustical properties suggested structure forming tendency of the polymer as confirmed positive values of S_n (Fig. 1). From Fig. 1,

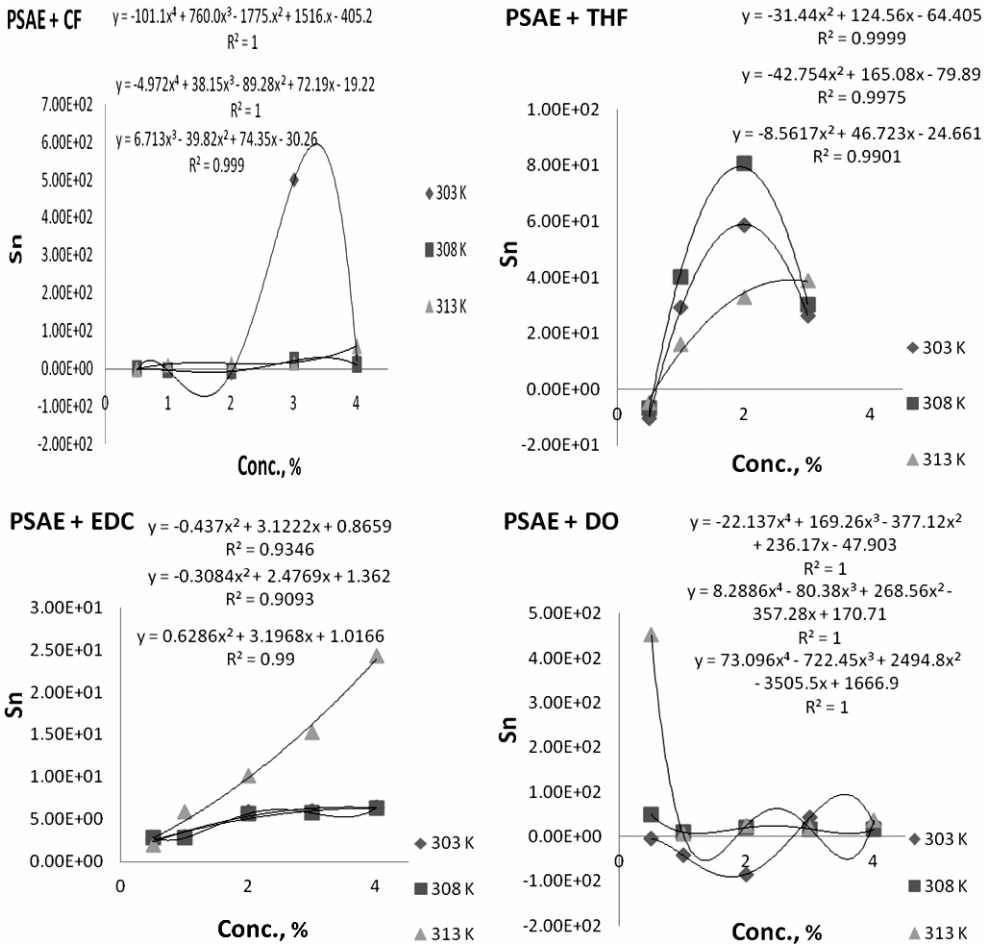

Fig. 1—The plots of Sn against C for PSAE at 303, 308 and 313 K in CF,DCE, THF and DO

it is observed that variation in S_n with C and T is nonlinear. In accordance to expected molecular interactions in solvent systems studied, the observed trend is CF > THF > DCE > DO. The decrease in S_n with C indicates predominant solute-solute interactions over solvent-solute interactions at a given temperature. Thus, dipole-dipole interactions of opposite type favored structure formation and that of the same type favored disruption of the structure formed previously. The structure forming tendency of the solute leads to modification of original structure, which may affect polymer processing from solutions and change in resultant dimensions of the article.

Conclusions

Various acoustical parameters have suggested existence of powerful molecular interactions in the solutions. PSAE has structure forming tendency in the studied solvent systems.

References

1 Pethrick, R. A., Acoustic studies of polymer solutions, J. Macromol. Chem. 9 (1973) 91-121.

2 Rajasekaran, J. F., Balakrishnan, R. and Arumugam, V., Internal pressure-free volume relationship for rubber solutions, J. Pure Appl. Ultrason. 19 (1997) 76-85.

3 Mason, T. J., The Uses of Ultrasounds in Chemistry, Royal Soc Chem Sonochemistry (1990).

4 Perpechko, I., Acoustical Methods of Investigating Polymers, Mir Publishers Moscow, 65 (1975).

5 Desai, J. A. and Parsania, P. H., Acoustical studies of cardo polysulfonates of 1,1'-bis (4-hydroxyphenyl) cyclohexane with 1,3-benzene disulfonyl chloride in different solvents at 30°C, J. Polym. Mater. 13 (1996) 79-83.

6 Kamani, M. M. and Parsania, P. H., Ultrasonic velocity studies of chloroform and dichloroethane solutions of cardopolysulfone of 1,1'-bis(3-methyl-4-hydroxyphenyl) cyclohexane and 4,4'-difluoro diphenyl sulfone, J. Pure Appl. Ultrasonic, 18 (1996) 46-54.

7 Kamani, M. M. and Parsania, P. H., Ultrasonic studies of chloroform-dioxane binary solutions of polysulfonate of 1,1'-bis(3-methyl-4-hydroxyphenyl) cyclohexane with toluene-2,4-disulfonyl chloride, J. Polym. Mater. 13 (1996) 191-194.

8 Shah, A. R. and Parsania, P. H., Synthesis, biological activity and chemical resistance of poly (4,4'-cyclohexylidene-R,R'-diphenylene-3,3'-benzophenone sulfonates), J. Polym. Mater. 14 (1997) 33-41.

9 Rajkotia, K. M., Baluja, S. and Parsania, P. H., Studies on acoustical properties of poly (4,4'-cyclopentylidene diphenylene-2,4-disulfonate) in different solvents at 30°C, Eur. Polym. J. 33 (1997) 1005-1010.

10 Shah, A. R. and Parsania, P. H., Acoustic properties of poly (4,4'-cyclohexylidene-R,R'-diphenylene-3,3'-benzophenonedisulfonates) at 30°C, Eur. Polym. J. 33 (1997) 1245-1250.

11 Desai, J. A. and Parsania, P. H., Ultrasonic studies of poly (1,1'-cyclohexylidenyl-4,4'-diphenylene-2,4-toluene disulfonate) solutions at 30°C, J. Pure. Appl. Ultrason. 19 (1997) 65-69.

12 Kamani, M. M. and Parsania, P. H., Ultrasonic studies of solutions of polysulfonate of 1,1'-bis(3-methyl-4-hydroxyphenyl)cyclohexane and toluene-2,4-disulfonyl chloride, J. Pure Appl. Ultrason. 19 (1997) 89-93.

13 Karia, F. and Parsania, P. H., Ultrasonic velocity studies and allied parameter of poly(4,4'-cyclohexylidene-R,R'-diphenylenediphenylmethane-4,4'-disulfonate) solutions at 30°C, Eur. Polym. J. 36 (2000) 519-524.

14 Patel, Y. V. and Parsania, P. H., Ultrasonic velocity study of poly(R,R',4,4'-cyclohexylidene diphenylene diphenyl ether-4,4'-disulfonate solutions at 30°, 35° and 40°C, Eur. Polym. J. 38 (2002) 1971-1977.

15 Manwar, B. G., Kavathia, S. H. and Parsania, P. H., Ultrasonic velocity study of poly (R, R', 4, 4'-cyclohexylidene diphenylene toluene-2, 4-disulfonates) solutions at 30°, 35° and 40°C, J. Pure Appl. Ultrason. 26 (2004) 49-57.

16 Vogel's Textbook of Practical Organic Chemistry, 5th edn (ELBS, London), (1991) 395-412.

17 Senthil, R. K. and Rakkappam, C., Acoustic studies on solvent-solute interactions in non-aqueous polymer solutions, Asian J. Phys. 6 (1997) 467-472.

18 Das, S., Singh, R. P. and Maiti, S., Ultrasonic velocities and Rao formulism in solution of polyesterimides. Polym. Bull. 2 (1980) 400-409.

19 Bell, W. and Pethrick, R. A., Ultrasonic investigations of linear and star shaped polybutadiene polymers in solutions of cyclohexane, hexane and ethylbenzene, Polym. 23 (1982) 369-378.

20 Vasoya, P. J., Mehta, N. M., Patel, V. A. and Parsania, P. H., Effect of temperature on ultrasonic velocity and thermodynamic parameters of cardo aromatic polysulfonate solutions, J. Sci. and Ind. Res. 66 (2007) 841-848.

21 Mehta, N. M., Karia, F. D. and Parsania, P. H., Effect of temperature on ultrasonic velocity and thermodynamic parameters of bisphenol-C-formaldehyde-acrylate resin solutions, Fluid Phase Equilibria, 262 (2007) 61-68.

22 Pethrick, R. A. and Poh, B. T., Ultrasonic attenuation and adiabatic compressibility of poly (ethylene oxide) water mixtures, British Polym. J. 15 (1983) 149-157.

J. Pure Appl. Ultrason. 34 (2012) pp. 90-92

Molecular interaction studies in aqueous antibiotic solution at different temperatures using ultrasonic technique

Sunanda S. Aswale[1*], Shashikant R. Aswale[1*], Rajesh S. Hajare[2]

[1]Lokmanya Tilak Mahavidyalaya, Wani, Dist. Yavatmal, (MS).

[2]Nilkanthrao Shinde College, Bhadrawati, Dist. Chandrapur, Maharashtra.

Email: sraswale@gmail.com; ssasale@rediffmail.com, rajeshhajare34@yahoo.com

The study of intermolecular interaction plays an important role in development of molecular sciences. The molecular interactions in liquids provide valuable information about the behavior of liquids and solutions. The thermodynamic and acoustical studies elucidate the nature of interaction between molecules in liquids and solutions. The study of propagation of ultrasonic waves in liquid systems is established as significant tool in determining the nature of interactions between molecules in liquids and solutions. The ultrasonic parameters are directly related to a number of thermodynamic parameters. The ultrasonic velocity, density and viscosity have been measured for aqueous solution of antibiotic ceftriaxone sodium at three different temperatures 303.15K, 308.15K and 313.15K and frequency 2MHz. The measured data have been used to compute the acoustical properties namely adiabatic compressibility, intermolecular free length, specific acoustic impedance, relative association, relaxation time, Rao's constant and Wada's constant. These thermodynamic, acoustical parameters are used to discuss the molecular interactions in aqueous solution of antibiotic ceftriaxone sodium.

Keywords: molecular interaction, acoustical parameters, ultrasonic velocity, ceftriaxone sodium

Introduction

The structure, nature and prevailing conditions of solvents and solutes play an important role on resulting properties and interaction occur in solutions. The field of ultrasonic fairly vast and apart from day to day applications it is widely used in Medical Ultrasonic next to x-ray, non-destructive testing, acoustics in buildings etc. Ultrasonic parameters provide valuable information in solutions. Ultrasonic waves are established an effective means for analyzing certain physical properties of the materials. The study of propagation of ultrasonic waves in liquid systems and solids is now rather well established.

In continuation of our work[1-4] in the present investigation the ultrasonic velocity, density and viscosity measurement of aqueous solution of ceftriaxone sodium at temperatures 303.15K, 308.15K and 313.15K and frequency 2MHz can be used to compute various acoustical parameters. The result obtained from these acoustical parameters interpreted on the basis of molecular interactions.

Experimental

Antibiotic drug ceftriaxone sodium obtained from prosperity 6 pharmaceutics limited was used. Double distilled water was used for making solutions. Densities were measured with the help of density bottle. Weighing was done on Roy CCB-4 Balance, (± 0.001 g). A special thermostatic water bath arrangement was made for density, viscosity and ultrasonic velocity measurements in which there is continuous stirring of water with the help of electric stirrer and temperature variation was maintained within ± 0.1°C. All the ultrasonic velocities were measured using a single crystal interferometer with accuracy of ± 0.03% and frequency 2 MHz The densities, viscosities and ultrasonic velocities of solvent water and 0.001 molar solution of ceftriaxone sodium were measured at temperatures 303.15K, 308.15K and 313.15 K.

Results and Discussion

In the present investigation, measurements of densities, viscosities and ultrasonic velocities of solvent water and an antibiotic ceftriaxone sodium solution have been made and given in Table- 1.

The adiabatic compressibility (β) is evaluated by using equation.

$$\beta = 1 / v^2.d \quad \ldots (1)$$

Specific acoustic impedance is determined from the measurement of ultrasonic velocity and density by formula,

$$Z = v_s \, . \, d_s \quad \ldots (2)$$

*Life member, Ultrasonics society of India.

Presented at National Seminar on Materials characterization by ultrasonic (NSMCU-2012), 3-4 April 2012, Amity school of Engineering & Technology, New Delhi

Relative association is a function of ultrasonic velocity and is calculated by the equation,

$$R_A = \left[\frac{d_s v_0}{d_0 v_s} \right] \quad \ldots (3)$$

where, v_0 and v_s are ultrasonic velocities in solvent and solution.

Intermolecular free length has been evaluated from adiabatic compressibility (β) by Jacobson's formula,

$$L_f = K\sqrt{\beta_s} \quad \ldots (4)$$

where, K is the temperature dependent constant known as Jacobson's constant and is independent of the nature of liquid. (at 303.15 K, K=631)

Relative Viscosity of Solution is calculated by equation

$$\eta_2 = \eta_1.t_2.d_s/t_1.d_0 \quad \ldots (5)$$

where, η_2 = viscosity of experimental liquid, η_1 = viscosity of water, t_1 = time flow of water, t_2 = time flow of experimental liquid, d_0 = density of water and d_s = density of experimental liquid.

Relaxation time is evaluated by equation

$$\tau = 4/3\beta.\eta \quad \ldots (6)$$

where, β = adiabatic compressibility η = viscosity of experimental liquid

Free volume is calculated by following equation

$$V_f = [M_{eff} v/K\eta]^{3/2} \quad \ldots (7)$$

where, M_{eff} is effective molecular weight, K is a temperature independent constant which is equal to 4.28×10^9 for all liquids.

Rao's constant is calculated by using following equation.

$$R = [M_{eff}/d_s]v^{1/3} \quad \ldots (8)$$

Wada's constant is calculated by following equation.

$$W = [M_{eff}/d_s]\beta^{-1/7} \quad \ldots (9)$$

The experimentally determine values are listed in Table -1.

Calculated adiabatic compressibility, acoustic impedance, relative association, intermolecular free length, relaxation time, free volume, Rao's constant and Wada's constant for aqueous solution of ceftriaxone sodium at different temperatures are given in Table-2 and 3.

From this data molecular interaction in aqueous solution of ceftriaxone sodium will be predicted.

A keen look at the Table 1, suggests that the experimentally calculated values of density and viscosity of aqueous solution of ceftriaxone sodium decreases where as ultrasonic velocity increases with increases in temperature. The increasing value of ultrasonic velocity with temperature shows strong attraction between the solute and solvent molecules. The decrease values of density and viscosity with increase in temperature shows decrease in intermolecular forces due to increasing the thermal energy of the system.

From the table 2 and 3, it reveals that the computed values of adiabatic compressibility, relative association, intermolecular free length, relaxation time and free volume decreases with increase in temperatures where as acoustic impedance, Rao's constant and Wada's constant increases. This non-ideal behavior of acoustical, thermodynamic parameters indicates strong intermolecular interactions between solute and solvent molecule of aqueous solution of ceftriaxone sodium. This reflects the

Table 1—Ultrasonic Velocities, densities and viscosities of 0.001M Ceftriaxone sodium Solution at different temperatures

Temperature (K)	Ultrasonic Velocity (m/s)	Density (kg/ m^3)	Viscosity $\times 10^{-3}$ (kg $m^{-1}sec^{-2}$)
303.15	1490.19	1025.40	0.8429
308.15	1523.91	1020.92	0.7508
313.15	1554.55	1015.52	0.6800

Table 3—Thermodynamic parameters of Ceftriaxone Sodium at different temperatures.

Temperature (K)	Free Volume $V_f \times 10^{-8}$ (m^3/mole)	Rao's Constant (R) (m^3/mole) $(m/s)^{1/3}$	Wada's Constant (W) (m^3/mole) $(N/m^2)^{1/7}$
303.15	1.30	0.2097	0.3986
308.15	1.13	0.2123	0.3947
313.15	1.00	0.2147	0.4020

Table 2—Acoustical parameters of 0.001M Ceftriaxone Sodium at different temperatures

Temperature (K)	Adiabatic Compressibility $\beta \times 10^{-10}$	Specific Acoustic Impedance $Z \times 10^4$ ($Kgm^{-2}sec^{-1}$)	Intermolecular free length (L_f)	Relative association (R_A)	Acoustic relaxation time $\tau \times 10^{-10}$sec
303.15	4.31	15.28	0.0131	1.0316	4.93
308.15	4.20	15.58	0.0129	1.0272	4.21
313.15	4.07	15.78	0.0128	1.0183	3.69

formation of hydrogen bond between solute and solvent molecule of aqueous solution of ceftriaxone sodium. This observation similar to that of liquid mixture where non-ideal behavior is attributed to strong intermolecular interactions[5, 6]. Anbanathan[7] and Ernst *et al.*[8], in their studies on liquid mixtures reported the non-ideal behavior due to the molecular association of water molecules. The variation of acoustical parameters in liquid mixture is attributed to strong intermolecular association between solute and solvent molecules[9, 10]. C. Roumana and *et al.*[11] in their studies of aqueous solution of cefadroxil reported non-ideal behavior attributed to strong intermolecular interactions.

The present investigation of aqueous solution of ceftriaxone sodium is in agreement with the reported observations, where strong intermolecular interaction reflects the hydrogen bond formation in aqueous solution of cefriaxone sodium.

Conclusion

The present study of aqueous solution of cefriaxone sodium shows non-ideal behavior of ultrasonic velocity and acoustic, thermodynamic parameters indicate strong intermolecular interaction on the basis of hydrogen bond formation in aqueous solution of cefriaxone sodium, which are responsible to drug absorption and transmission at higher temperatures.

References

1 S. S. Aswale, S. R Aswale, D. T. Tayade, and P.B. Raghuwanshi, Apparent molar compressibility Specific acoustic impedance of α-bromoacetophenone and Coumaran-3-ones in ethanol and dioxane solvent, J. pure appl.Ultraso, 30, 2008, 62.

2 S. S. Aswale, A. B. Dhote, R. S. Hajare, P. B. Raghuwanshi, and S. R. Aswale, Use of ultrasonic velocity to study solute-solvent interaction of Coumaran-3-ones in polar and non-polar solvents, Proceedings of Eighteenth National Symposium on Ultrasonics, **NSU-XVIII, 2009,** Vellore, 2009, 132.

3 S. R. Aswale, S. S. Aswale, A. B. Dhote, and D. T. Tayade, Ultrasonic investigation of molecular interaction in Paracetamol solution at different concentration, J. Chem. Pharm. Res. (6), 2011, 233.

4 S.S. Aswale, P.B. Raghuwanshi, D.T. Tayde and S.R. Aswale, Comparative study of intermolecular interactions by acoustic properties of α-bromoacetophenone and Coumaran-3-ones in ethanol and dioxane solvent, J. Indian Chem. Soc., 84, 2007, 159.

5 A. Dhanlaxmi and S. Sekar J. Acoust. Soc. Ind., 13(2), 1995, 66-71.

6 S. Naidu, and R. Prasad, K., Molecular interaction in binary mixture of tenvalerate, J. Pure Appl. Ultrason., 27, 2005, 15-24.

7 D. Anbanathan, J. Acoust. Soc. India, 4, 1974, 123.

8 S. Ernst, and Jezowska Trzebiatowska, B. Phys. Chem., LPZ, 2, 256.

9 V. D. Bhandarkar, V. A. Tabhane and S. Ghosh, Ultrasonic study of molecular interactions in binary liquid mixtures: acrolien and cinnamaldehyde in methanol, cyclohexane and p-diaxane, Indian J. of pure and Appl. Phys., 41, 2003, 849-854.

10 I. Vibhu, A. Misra, M. Gupta and J. Shukla, Ultrasonic and infrared study of molecular interactions in ternary mixtures of 1-napthol and 2-naphthol with 2-propanone in benzene, Pramana, 62 (5), 2004, 1147.

11 C. Roumana, G. Velraj. Roumaisa, M. G. Mohammed Kamil, Acoustical investigation of molecular interaction in aqueous antibiotic solution, J. pure Appl. Ultrason, 30, (2008) 97.

J. Pure Appl. Ultrason. 34 (2012) pp. 93

PhD Thesis Summary

Behavioral Study of Ultrasound Wave Propagation in Biological Tissues

(Awarded 2011 by I.I.T. Roorkee to Narendra D. Londhe, N. I. T Raipur)

The biological tissue has a complex structure which shows an unpredictable behavior for ultrasonic waves. The acoustical properties of various tissues are different and phenomenon like scattering diffraction, attenuation and nonlinearity. The nonlinearity leads to the distortion of the transmitted beam while spreading energy in higher harmonics, and images are acquired preferably by receiving those of second harmonic, known as tissue harmonic imaging (THI). The harmonic image often demonstrates improved contrast resolution due to higher harmonic frequencies and therefore detects smaller objects. High frequencies are, however, attenuated more in biological tissues as the beam propagates, leading to reduced depth of penetration inside the objects under scan. A new imaging technique named "super-harmonic imaging" (SHI) has been proposed recently. It takes advantage of the higher harmonics (third to fifth) arises from nonlinear propagation. It provides further enhancement in resolution with acceptable penetration depth and signal-to-noise ratio (SNR). The dedicated phased array transducer and propagation model that enables the full exploitation of SHI are the topics of ongoing research.

The study starts with the derivation of nonlinear wave equation. This is further modulated to Burger's equation which has only attenuation and nonlinearity terms. Burgers' equation is used to model the nonlinear propagation of single sinusoidal wave with finite amplitude. The analytical solution for Burger's equation is also compared with time domain solution of modified KZK equation in which the diffraction term is removed. With the same methodologies, THI and SHI analysis has been done along axial axis. The SNR and penetration depth both have improved for superharmonic field.

In the next study, we have combined time and frequency domain methods by using time domain solution of Burger's equation to solve nonlinearity and frequency domain solution for diffraction and attenuation. The simulation is performed for conventional short Gaussian pulse from phased array transducer. The lateral and axial views of field propagation confirm the harmonic generation and found in excellent agreement with analytical solution of Burger's equation.

Another numerical representation based on the Neumann iterative method combined with a Green's function approach as an algorithm to compute nonlinear wave propagation has been studied. The method is validated for a one-dimensional nonlinear wave problem. We have evaluated the wavefield, including harmonic frequencies up to the fifth harmonic. The results are compared with a solution of the lossless Burgers' equation and found in perfect agreement.

Further, we have used amplitude modulated and frequency modulated excitations altogether to study their effects on THI and SHI. The results have been obtained using the above mentioned nonlinear models. The effects of imaging system's parameter variation on the evaluation parameters like beamwidth, off-axis level, side-lobe level etc are calculated and compared for fundamental, second harmonic and superharmonic components. Again the transducer parameters variation has been done and its effect on beam pattern and trade-off between image quality parameters has been thoroughly investigated for optimized superharmonic beam.

Lastly, most widely used coded excitations in radar system such as linear and nonlinear frequency modulated waves have been used. The simulations are based on pseudospectral model for nonlinear propagation and processing is done in MATLAB. The similar study is also done using the composite time-frequency domain algorithm for LFM and NLFM excitations. It has also been computationally checked and confirmed that coded excitations provides better SNR, resolution and penetration depth in second and superharmonic imaging as compared to the conventional excitations. Thus, this study has shown the new phase in ultrasound imaging i.e. coded superharmonic imaging (CSHI).

Author Index
Volume 34, January-December 2012